A TALE OF TWO STANDARD MODEL EXTENSIONS

by

DESMOND VILLALBA

NOBUCHIKA OKADA, COMMITTEE CHAIR
ALLEN STERN
CONOR HENDERSON
GEORG SCHWIETE
KAUSTUBH AGASHE

A DISSERTATION

Submitted in partial fulfillment of the requirements
for the degree of Doctor of Philosophy
in the Department of Physics and Astronomy
in the Graduate School of
The University of Alabama

TUSCALOOSA, ALABAMA

2019

ABSTRACT

The Standard Model (SM) has provided physicists with a nearly complete effective description of the fundamental building blocks for the Universe. While several questions regarding the makeup of our Universe have been resolved, many still remain. One such question deals with the vast energy difference between the electroweak scale and Planck scale ($\mathcal{O}(10^{17}\,\text{GeV})$). The origin of this large divide has physical implications affecting the running of the Higgs mass, as it receives quantum corrections that are quadratic. Affiliated with this large division of energy scales is an issue that came about upon detection of the Higgs boson at the Large Hadron Collider (LHC), which enabled us to infer the value of the Higgs self-coupling. As a result, the renormalization group equation for the Higgs self-coupling predicts a negative self-coupling at around energies of $10^9 - 10^{11}$ GeV. If true, this would indicate that our vacuum state is unstable. Taking our motivation from stringy effects by modifying the local kinetic term of an Abelian Higgs field by the Gaussian kinetic term, we show that the Higgs field does not possess any instability, and the beta-function of the self-interaction for the Higgs becomes exponentially suppressed at high energies, showing that such class of theory never suffers from a vacuum instability. Another interesting question to consider, is what might be the origin of the large mass difference between the fundamental fermions? As will be shown, the fermion mass hierarchy can be explained through the use of our formalism developed in our setup of the "Domain-Wall Standard Model in a non-compact 5-dimensional space-time", where all the SM fields are localized in certain domains of the 5th dimension. Reproducing the hierarchy is contingent upon the localization positions of the fermions along the extra flat dimension. As a result of these different localization points, the effective 4-dimensional Kaluza-Klein mode gauge couplings become non-universal. This allows for the possibility of interesting experimental

considerations which will be discussed. Flavor Changing Neutral Current constraints provide stringent bounds on our model, through these constraints we can glean information about the extra dimension. We have found two possibilities that satisfy these constraints: (1) the KK mode of the SM gauge bosons are extremely heavy and unlikely to be produced at the LHC, however future FCNC measurements can reveal the existence of these heavy modes. (2) the width of the localized SM fermions is very narrow, meaning the 4D KK mode gauge couplings are almost universal. In this case the FCNC constraints can be easily avoided, even for a KK gauge boson mass of order TeV. Such a light KK gauge boson can be discovered at the LHC in the near future.

DEDICATION

I dedicate this work to my wonderful wife Meredith, who has been a great emotional support along the way through her love and her ability to keep me laughing. To my mother Tammy, who always pushed me to do more and follow whatever my passions were. To my sisters Jessika and Brittanie, whose love and support I feel no matter the distance between us. Lastly, to my father Fred, who helped plant the seed for my interest in science and technology a long time ago.

ACKNOWLEDGMENTS

I would first like to thank my adviser Prof. Nobuchika Okada, for his patience in teaching me and his willingness to share his knowledge on a variety of topics. Through his mentorship I have expanded my understanding of the world exponentially, and for that I am eternally grateful. In addition, I would like to thank and acknowledge my collaborators Digesh Raut, Anupam Mazumdar, and Anish Goshal. I would also like to thank the members of my thesis committee, Prof. Allen B. Stern, Prof. Conor Henderson, Prof. Georg Schwiete, and Prof. Kaustubh Agashe, for all of their guidance and suggestions. I would also like to thank Prof. Ryoichi Kawai from UAB, who always helped me and provided numerous interesting discussions on a variety of physics topics. Lastly, I would like to thank Prof. Sarah Formica and Prof. Richard Prior from UNG for their guidance and support during my undergraduate years.

CONTENTS

LIST OF TABLES

LIST OF FIGURES

CHAPTER 1

INTRODUCTION

The Standard Model (SM) of particle physics is a near-complete effective description of the fundamental underpinnings of our Universe. Construction of the SM is primarily reliant on the concept of symmetry. The Lagrangian of the SM must posses certain local and global symmetries, or in other words, the Lagrangian must be invariant under transformations linked to these symmetries. One of the most fundamental of symmetries, the Lorentz invariance, dictates that physics remains the same in any orientation or frame of reference. Transformations that affect internal degrees of freedom, but leave the overall Lagrangian invariant are known as gauge symmetries. The presence of these gauge symmetries necessitates the presence of force mediators or vector bosons, and are largely responsible for holding the matter around us together today.

The total gauge group of the SM is a combination of Non-Abelian and Abelian gauge groups and is given by $SU(3)_C \otimes SU(2)_L \otimes U(1)_Y$, where the first group represents the strong interactions and the latter two are responsible for the electroweak interactions. Quantum Chromo Dynamics describes the interactions between the massless strong force carries, the gluons and the massive quarks. The electroweak interactions represent one of the first examples of the unification of fundamental forces, in this case the electromagentic and the weak nuclear forces. The force carries for the weak force are the massive $W^{\pm}$ and Z^0 bosons, and the massless photon, often represented by γ mediates the electromagnetic force. All of the vector bosons have a spin of $l = 1$. The strength of the interactions between the vector bosons and matter is controlled by the *coupling strength* for each gauge

	$\mathrm{SU}(3)_C$	$\mathrm{SU}(2)_L$	$\mathrm{U}(1)_Y$
q_L^i	**3**	**2**	$1/6$
u_R^i	**3**	**1**	$2/3$
d_R^i	**3**	**1**	$-1/3$
ℓ_L^i	**1**	**2**	$-1/2$
e_R^i	**1**	**1**	-1
H	**1**	**2**	$-1/2$

Table 1.1: The particle content of the SM.

group. Due to quantum effects, these couplings' values vary with energy. The strong force is *strong* because of its large coupling g_S, which tends to non-perturbative behavior in the low energy or infra-red (IR) energy regime. On the other hand, the weak coupling g_L and hypercharge g_Y couplings are comparable one another over most of the energy range. The origin of the designation of the term "weak force" is dubbed so, not because of an exceptionally small coupling, but the massive nature of the $W^{\pm}$ and Z^0 vector bosons that mediate this force. Their mass has been measured to be around $M_W = 80$ GeV and $M_Z = 91$, GeV respectively. Since the photon remains massless, interactions with electrically charged matter are more pronounced than the weak interactions.

So far, the fundamental matter content we have been able to detect consists of the fermions of spin $l = 1/2$, and most recently the Higgs boson of spin $l = 0$. The fermions of the SM consist of the quarks: up, down, charm, strange, top, bottom and the leptons: electron, muon, tau, and their respective neutrinos. Interestingly, our universe distinguishes between different spin orientations or *handedness*, requiring further classification into left-handed and right-handed chiralities. This classification divides the SM constituents into different representations of the gauge groups as shown in Table1.1, thereby affecting how the SM matter contents interact with the vector bosons. The Higgs boson was discovered in 2012 at the LHC [1, 2], with a mass around $m_H = 125$ GeV, and was one of the final missing pieces to the SM. The Higgs is an essential component to the SM for several reasons, chief among them is that through the Higgs mechanism, it provides mass to the $W^{\pm}$ and Z^0 vector bosons and fermions. As the only scalar in the SM, it

permits a potential term in the Lagrangian which is at the heart of the spontaneous symmetry breaking (SSB), that ultimately leads to the electroweak symmetry breaking and produces the SM mass spectrum (see Ref [3] for a review).

Though the SM has proved to be an excellent effective description of nature, there are several experimental and observational measurements, as well as conceptual difficulties that cannot be explained with the SM alone. These beyond the standard model (BSM) explanations attempt to cobble together the SM with either new symmetries, particles, or other extensions in an attempt to connect known measurements to the new physics being detected or inferred. The primary deficiencies of the SM that are actively being pursued today include: the absence of neutrino mass description, an explanation for dark matter (DM), and incorporating a quantum description of gravity. Below these glaring deficiencies lie several slightly less infamous issues or "problems", two of which will be addressed in this dissertation.

The first problem investigated deals primarily with the *hierarchy problem*, that is, what could be an explanation for the vast difference in fundamental energy scales? The difference in energy between the electroweak scale and the Planck scale is 17 orders of magnitude! This question has physical implications affecting the running of the Higgs mass, as it always receives corrections that are quadratic. If there is no new physics to mitigate this behavior, the Higgs mass will grow quadratically up to the Planck scale $M_{Planck} \approx 10^{19}$ GeV (see Refs.[4, 5, 6] for a review). Several propositions haven been devised to either remove or sidestep the hierarchy problem, such as supersymmetry [7], technicolor [8], and compact extra dimensions [9] to name a few. Each of these proposed solutions have their own merits, and have either evolved over the years in order to fit experimental data or been ruled out almost entirely.

Related to this problem is the instability of the Higgs vacuum. This instability manifests due to the quantum corrections to the Higgs self-coupling around an energy scale of 10^{11} GeV. Near this energy, the Higgs self-coupling runs negative due to its interaction

with the relatively large top quark Yukawa coupling. The result of this behavior at high energies invites the possibility of an even lower, more energetically favorable vacuum. This would of course throw our current Universe askew, as all fundamental particles in the SM acquire their mass from the interaction with the Higgs vacuum expectation value (VEV). Fortunately, it seems that the decay time to this lower energetic state is longer than the age of the Universe. Though the exact details are still debated, this fascinating issue has been closely studied for at least the past 4 decades and counting (see Refs. [10, 11, 12, 13]). According to the measured values of the Higgs and top quark masses, our Universe seems to exist in a long-lived metastable state. The leading assumption in this metastable configuration is that only SM interactions can influence the Higgs potential, as all new physics are believed to be suppressed by the Planck scale. Based on arguments in [13], however, perhaps this assumption is a bit naive. Nevertheless, the main culprit of the instability seems to be due to the negative running of the self-interactions at high energy scales.

Our proposed resolution to the gauge hierarchy problem in Ref. [14] involves invoking a new scale (on the order of 10^5 GeV) which is motivated by string field theory, and employs a modification to the kinetic operator with an infinite derivative expression (for a review see Refs. [15, 16, 17, 18, 19, 20, 21, 22, 23, 24]). The exact form of the modification does not appear to be unique, and as long as the expression is an *entire function*, no ghosts will appear in the theory. Our choice for the infinite derivative function is a gaussian exponential, which suppresses ultraviolet (UV) behavior. The general effect on the SM is unseen at low energies, whereas the loop corrections are all effectively switched off above the new so-called "non-local scale" M. The meaning of the term "non-local" (NL) becomes apparent in the following example for a real scalar field. The canonical commutation relation in the NL setup is

$$[\phi(t,\mathbf{x})_{NL}, \pi(t,\mathbf{y})_{NL}] = \frac{i}{\pi^{3/2}\left(\frac{1}{M^3}\right)} e^{\frac{-(\mathbf{x}-\mathbf{y})^2}{4\left(\frac{1}{M^2}\right)}}, \tag{1.1}$$

where ϕ ($\pi = \dot{\phi}$) is the scalar (scalar canonical momenta) operator. This relationship indicates that as a result of the NL extension, particles are "smeared out" in space. In the local limit ($M \to \infty$), the usual commutation relationship is attained

$$[\phi(t, \mathbf{x})_{NL}, \pi(t, \mathbf{y})_{NL}]\Big|_{M\to\infty} = [\phi(t, \mathbf{x}), \pi(t, \mathbf{y})] = i\delta^3(\mathbf{x} - \mathbf{y}). \tag{1.2}$$

Through calculations of the modified β functions, we've shown that the Higgs field does not possess any instability. The Yukawa coupling between the scalar and the fermion, the gauge coupling, and the self interaction of the Higgs are all exponentially suppressed running at high energies, showing that such class of theory never suffers from vacuum instability.

The second problem to be discussed deals with the large mass/energy divide between the SM fermions. The top quark's measured mass of $m_t = 173$ GeV [27] dwarfs the masses of the neutrinos, which are most recently estimated to be around $m_\nu \approx 5 \times 10^{-11}$ GeV [28]. What could be an explanation behind the hierarchy present among the fundamental fermions? One possibility is that the Yukawa couplings between the neutrinos and the Higgs field is very small. If we assume the right-handed neutrinos added to the SM are Dirac type fermions, then the Yukawa couplings would need to be around $Y_\nu \approx 10^{-12}$. As compared to the other SM fermions' Yukawa couplings, this minuscule neutrino Yukawa coupling is less theoretically appealing, or considered "unnatural". A class of explanations designed to explain the smallness of the neutrino mass, also known as the *seesaw mechanism*, provide several compelling reasons behind why their masses are so small (see [29] for a review).

Despite the successes of the seesaw mechanism in explaining the smallness of the neutrinos' masses, there is still a lacking in the understanding behind the mass hierarchy overall. A drastically different approach that has been more recently devised, considers the effects of extra-dimensions on the SM. In these extra-dimensional theories, the "geometry" of the setup provides us with a novel prospect of understanding the mysteries within the SM through several phenomenology considerations. The large extra-dimension model [9] is

a well-known brane-world scenario which offers a solution to the gauge hierarchy problem by diluting the Planck scale to the TeV scale by a large extra-dimensional volume that is on the order of $\mathcal{O}(0.1\,mm)$. Another well-known scenario is the warped extra-dimension model [30], where the Planck scale is warped down to the TeV scale in the presence of the anti-de Sitter (AdS) curvature in the extra 5th dimension. Through the introduction n extra-dimensions and with the use of "geometry", the authors in Ref. [31] show that the origin behind the fermion masses could be due to the localization positions of the fermions in n extra-dimensions.

We build upon progress in this direction and propose a framework to construct the "Domain-Wall Standard Model" (DWSM) in a non-compact 5-dimensional space-time in Refs. [32, 33, 34], where all the SM fields are localized in certain domains of the 5th dimension and the SM is realized as a 4-dimensional (4D) effective theory without any compactification for the 5th dimension. This direction has been considered in Ref. [35] before, where the SU(5) gauge symmetry is introduced in the 5D bulk and the Dvali-Shifman mechanism [36] is assumed for dynamically localizing the SM gauge bosons associated with the breaking of the SU(5) gauge symmetry down to the SM gauge group. We consider a simpler approach to localize a gauge field in the bulk without extending the SM gauge groups, which has been proposed in Ref. [37]. We use the same mechanism for the localization of the SM Higgs field, while the SM fermions are localized via the mechanism proposed in Ref. [38] (DW fermion). The mass hierarchy can be naturally explained by suitably distributing the fermions in different positions along the extra dimension. Due to these different localization points, the effective 4D Kaluza Klein (KK) mode gauge couplings to the SM fermions become non-universal. As a result of the non-universal couplings, our model is severely constrained by the Flavor Changing Neutral Current (FCNC) measurements. We have found two possibilities that satisfy these constraints: (1) the KK-mode of the SM gauge bosons are extremely heavy and unlikely to be produced at the Large Hadron Collider (LHC), however future FCNC measurements

can reveal the existence of these heavy modes. (2) the width of the localized SM fermions is very narrow, meaning the 4D KK-mode gauge couplings are almost universal. In this case the FCNC constraints can be easily avoided, even for a KK gauge boson mass of order TeV. This light KK gauge boson can be discovered at the LHC in the near future.

This organization of this thesis is as follows. The main body of this thesis is a compilation of four of my works, and is split between two major BSM questions: (1) can the gauge hierarchy be resolved, and (2) what could be an explanation behind the origin of the SM fermion masses? Chapter 2 corresponds to my work [14] entitled "*On the Stability of the Infinite Derivative Higgs*" in collaboration with A. Goshal, A. Mazumdar, and N. Okada. The gauge hierarchy problem and Higgs vacuum instability can be resolved by the introduction of modified kinetic operators, which results in highly suppressed quantum corrections beyond the non-local scale M. Chapter 3 corresponds to my work [32] entitled "*Domain-Wall Standard Model in non-compact 5D and LHC phenomenology*" in collaboration with D. Raut and N. Okada. In a non-compact 5D space-time, where all of the SM fields are localized in certain domains of the 5th dimension and the SM is realized as a 4D effective theory without any compactification for the 5th dimension. Chapter 4 corresponds to my work [33] entitled "*Aspects of Domain-Wall Standard Model*" in collaboration with D. Raut and N. Okada. Two simple solvable examples which lead to domain-wall configurations for the SM particles and their KK modes are introduced. With these examples, a variety of phenomenologies of the Domain-Wall are investigated; such as the KK-mode gauge boson phenomenology at the LHC, and the effect of the KK-mode SM fermions on Higgs boson phenomenology. Chapter 5 corresponds to my work [34] entitled "*Fermion Mass Hierarchy and Phenomenology in the 5D Domain Wall Standard Model*" in collaboration with D. Raut and N. Okada. The mass hierarchy can be naturally explained by suitably distributing the fermions in different positions along the extra dimension. Due to these different localization points, the effective 4D KK-mode gauge couplings to the SM fermions become non-universal. These non-universal effective gauge couplings introduce

tree-level FCNC effects, which are highly constrained from the meson oscillation measurement data. As a result of these constraints, interesting phenomenology is considered. Chapter 6 is a summary of the all of the above works.

CHAPTER 2

ON THE STABILITY OF INFINITE DERIVATIVE ABELIAN HIGGS

2.1 Introduction

One of the key aspects of quantum field theory is to remove the ultraviolet (UV) divergences as in the case of quantum electrodynamics. In the context of Standard Model (SM), however, this leads to the *well-known* hierarchy problem for the SM Higgs [6]. The *key* observation is that the bosonic and the fermionic loop corrections to the Higgs mass and the self-interacting term yields an opposite effect, which does not cancel exactly, but leads to seventeen-orders of magnitude difference between the electroweak scale and the Planck scale. Furthermore, negative running of the self-interacting term for the SM Higgs gives rise to a metastable vacuum roughly at 10^{11} GeV, depending on the pole mass of the top-quark at the electroweak scale, see [25].

Indeed, there are many solutions to this problem including that of supersymmetry at low scales, see [6]. Here, we aim to address these problems not by introducing new states closer to the electroweak scale, but by invoking inherently another new scale motivated by string field theory by modifying the kinetic operator of the field with infinite derivatives [15, 16, 17, 18, 19, 20, 21, 22, 23, 24]. Such infinite derivatives indeed soften the UV behaviour, if they are captured by an *exponential of an entire function* [26]. First of all, exponential of an entire function does not introduce new poles in the propagator, therefore no new degrees of freedom arises in the spectrum [39, 40]. The propagator is exponentially suppressed in the UV, which helps softening the UV quantum behaviour.

In fact, it has been recently noticed in the context of gravity that an infinite derivative gravity, the gravitational interaction becomes weak at short distances and small time scales, such that the Big bang Singularity is now replaced by the Big bouncing, non-singular, cosmology, see [39, 40]. Furthermore, there is also no blackhole type singularity, because gravitational interaction can be weakened at a macroscopic scale of Schwarzschild's radius [41], while recovering the Newtonian $1/r$-fall at large distances from the source [40, 42]. Such theories also behave better in the quantum aspect, see [43, 44, 45], where infinite derivative gravity becomes finite in the UV. Similarly, modifying the kinetic term for the scalar, fermionic, and gauge field theory [26] have been studied in the past, see [46, 47, 48, 49, 50, 51, 52, 53].

The aim of this chapter is to show that in the case of an Abelian Higgs model the presence of *infinite derivatives* in the kinetic term yields all the β-functions to become exponentially suppressed in the UV. Indeed, this is one promising way to ameliorate the stability problem of the SM Higgs, because both Abelian and SM Higgs share similar interactions and properties. Towards the end we will comment on non-Abelian structure as well.

2.2 A simple toy model

In order to illustrate this, let us first consider a simple scalar toy model with ϕ being a real scalar and ψ being a Dirac fermion, the Lagrangian is [26],

$$\mathcal{L} = -\frac{1}{2}\phi e^{\frac{\Box+m_\phi^2}{M^2}}\left(\Box + m_\phi^2\right)\phi + \bar{\psi}e^{\frac{\Box+m_\psi^2}{M^2}}\left(i\gamma^\mu\partial_\mu - m_\psi\right)\psi - \frac{\lambda}{4!}\phi^4 - y\phi\bar{\psi}\psi. \tag{2.1}$$

where $\Box = \eta_{\mu\nu}\partial^\mu\partial^\nu$ $(\mu,\nu = 0,1,2,3)$ with the convention of the metric signature $(+,-,-,-)$, m_ϕ and m_ψ are the masses of the scalar and the Dirac fermion, respectively, and M is a scale of the non-locality which is taken to be below Planck scale. In our non-local field theory, only the kinetic terms are modified with the non-local scale M, while

the scalar self-interaction and the Yukawa interaction are the standard one. The theory is reduced into the standard local field theory in the limit of $M \to \infty$. In the Euclidean space ($p^0 \to ip^0_E$) the scalar and fermion propagators are given by [26]:

$$\Pi_\phi(p_E) = -\frac{ie^{-\frac{p_E^2+m_\phi^2}{M^2}}}{p_E^2+m_\phi^2},\ \Pi_\psi(p_E) = -\frac{i\not{p}_E e^{-\frac{p_E^2+m_\psi^2}{M^2}}}{p_E^2+m_\psi^2}\,. \tag{2.2}$$

Note that the non-local extension of the theory leads to the exponential suppression of the propagators for $p_E^2 > M^2$, and this fact indicates that quantum corrections will be frozen at energies higher than M. Since the mass terms for the scalar and fermion fields are irrelevant to our discussion, we drop them in the following analysis.

Let us now consider renormalization group (RG) evolutions of the couplings λ and y. The one-loop β-function for λ is of the form,

$$\mu\frac{d\lambda}{d\mu} = \beta_\lambda^{(1)} = f_{\lambda\lambda}\lambda^2 + f_y y^4 + f_{\lambda y}\lambda y^2, \tag{2.3}$$

where μ is the renormalization scale, $f_{\lambda\lambda}\lambda^2$ and $f_y y^4$ are due to the quantum corrections to the self-interaction vertex through scalar and fermion loop diagrams, respectively, while $f_{\lambda y}y^2\lambda$ is from the wave function renormalization of ϕ (anomalous dimension). In the standard quantum field theory (QFT), $f_{\lambda\lambda}\lambda^2$ and $f_y y^4$ can be extracted from the coefficients of logarithmic divergences of the 4-point 1-PI function in the loop-integrals. Although the propagators are modified in our present scenario, we adopt this standard procedure, in order to recover the standard QFT results in the limit of $M \to \infty$. Setting all external momenta to be zero, the 4-point 1-PI function is given by

$$\begin{aligned}\Gamma_4 &= -\frac{3}{2}\lambda^2\int\frac{d^4k_E}{(2\pi)^4}\left(\Pi_\phi(k_E)\right)^2 - 6y^4\int\frac{d^4k_E}{(2\pi)^4}\,\mathrm{tr}\left[\left(\Pi_\psi(k_E)\right)^4\right] \\ &= \int^{\Lambda^2} dk_E^2\left(\frac{3\lambda^2}{32\pi^2}\frac{e^{-2\frac{k_E^2}{M^2}}}{k_E^2} - \frac{24y^4}{16\pi^2}\frac{e^{-4\frac{k_E^2}{M^2}}}{k_E^2}\right),\end{aligned} \tag{2.4}$$

where we have introduced a cutoff scale Λ for the loop-integral in the Pauli-Villars regularization scheme.[1] According to the standard QFT procedure, we extract the β-function from Γ_4 by taking $\partial/\partial \log \Lambda$ and replacing the cutoff into the renormalization scale μ:

$$f_{\lambda\lambda}\lambda^2 + f_y y^4 = \Lambda \frac{\partial}{\partial \Lambda}\Gamma_4 \bigg|_{\Lambda\to\mu} = \frac{3\lambda^2}{16\pi^2} e^{-2\frac{\mu^2}{M^2}} - \frac{48y^4}{16\pi^2} e^{-4\frac{\mu^2}{M^2}}. \tag{2.5}$$

Note that the β-function is vanishing for $\mu > M$, while it retains the usual form upon taking $M \to \infty$ as we required. The power of the exponent $\left(\exp\left[-\mu^2/M^2\right]\right)^n$ is determined by the number of propagators running in the loop diagrams.

With an external momentum p_E in the Euclidean space, the 2-point 1-PI function is given by

$$\Gamma_2 = y^2 \int \frac{d^4k_E}{(2\pi)^4} \operatorname{tr}\left[\Pi_\psi\left(k_E\right)\, \Pi_\psi\left(k_E + p_E\right)\right] \tag{2.6}$$

Since the non-local extension involves quit a non-trivial p_E dependence for the loop-integral, the wave function renormalization term is more cumbersome to calculate, though we expect in the high energy limit ($\mu^2 \gg p_E^2$), the effect of the external momentum on the correction is negligible and we find

$$f_{\lambda y}\lambda y^2 = 4\lambda\gamma_\phi \approx \frac{8\lambda y^2}{16\pi^2} e^{-2\frac{\mu^2}{M^2}}, \tag{2.7}$$

where γ is the anomalous dimension for the scalar filed ϕ. For reader's convenience, we present detailed calculations of the anomalous dimension in Appendix A. Since the wave function renormalization is also exponentially suppressed, the field itself is completely frozen at energies higher than M.

[1] Pauli-Villars scheme is to show the connection between conventional QFT and our non-local case, based on our criterion that the conventional QFT result must be recovered in the limit of M $\to \infty$. However, loop-integral between μ and $\mu + \delta\mu$ can also be considered to perform the integrals since the integrals do not diverge due to the exponential softening.

Now we have found the β-function for $\mu > M$ is modified and approximately given by

$$\beta_\lambda^{(1)} \approx \frac{1}{16\pi^2}\left(3\lambda^2 + 8\lambda y^2\right) e^{-2\frac{\mu^2}{M^2}}. \tag{2.8}$$

Very interestingly, the β-function is vanishing towards high energies, and therefore the theory approaches a conformal field theory in the UV limit. In the view point of the vacuum stability, the dangerous correction factor f_y, which ordinarily drives the running $\lambda(\mu)$ to become negative, have become tamed and ultimately irrelevant in the UV limit. Hence, the non-local modifications to the quantum corrections provides a pathway to remedy the Higgs vacuum instability problem in the Standard Model!

Similarly, for the Yukawa interaction, we calculate the β-function for the Yukawa coupling (y),

$$\mu\frac{dy}{d\mu} = \beta_y^{(1)} = (f_w + f_v)\, y^3, \tag{2.9}$$

where $f_w y^3$ is from the wave function renormalizations for the scalar and the fermion, while $f_v y^3$ is from one-loop corrections to the 3-point 1-PI function. Setting all external momenta to be zero, the 3-point 1-PI function is given by

$$\Gamma_3 = iy^3 \int \frac{d^4k_E}{(2\pi)^4}\Pi_\phi(k_E)\ (\Pi_\psi(k_E))^2 = \frac{y^3}{16\pi^2}\int^{\Lambda^2} dk_E^2 \frac{e^{-3\frac{k_E^2}{M^2}}}{k_E^2}, \tag{2.10}$$

so that

$$f_v y^3 = \Lambda\frac{\partial}{\partial\Lambda}\Gamma_3\Big|_{\Lambda\to\mu} = \frac{2}{16\pi^2}y^3 e^{-3\frac{\mu^2}{M^2}}. \tag{2.11}$$

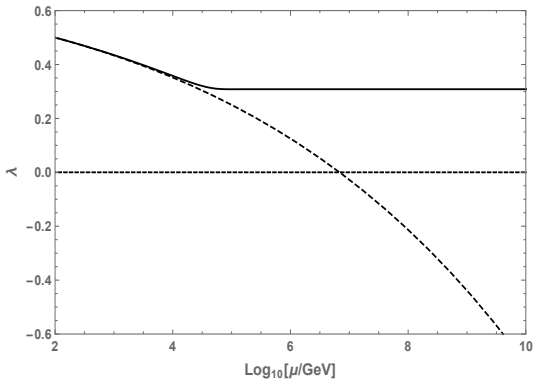

Figure 2.1: The scalar self-coupling running is shown in solid (dashed) black lines for the non-local (local) behavior. Here, we have taken initial values $\lambda = 0.5$ and $y = 0.6$ at $\mu = 100$ GeV, and the non-local scale to be $M = 10^5$ GeV.

The anomalous dimension for the fermion is calculated in Appendix B, and we obtain

$$\begin{aligned} f_w y^3 &= y\left(\gamma_\phi + 2\gamma_\psi\right) \approx \frac{y^3}{8\pi^2} y^3 e^{-2\frac{\mu^2}{M^2}} + \frac{y^3}{32\pi^2} y^3 e^{-2\frac{\mu^2}{M^2}} \\ &= \frac{3}{16\pi^2} y^3 e^{-2\frac{\mu^2}{M^2}}. \end{aligned} \tag{2.12}$$

Thus, we have found the β-function for $\mu > M$ is modified and approximately given by

$$\begin{aligned} \beta_y^{(1)} &\approx \frac{3}{16\pi^2} y^3 e^{-2\frac{\mu^2}{M^2}} + \frac{2}{16\pi^2} y^3 e^{-3\frac{\mu^2}{M^2}} \\ &\approx \frac{3}{16\pi^2} y^3 e^{-2\frac{\mu^2}{M^2}} \end{aligned} \tag{2.13}$$

The Yukawa coupling running also behaves in the similar manner to the running of $\lambda(\mu)$, where its β-function vanishes toward high energies.

In Figure 2.1, we show the RG evolution of the scalar self-coupling in the non-local theory (solid line), along with the one in the standard theory (dashed line). Here, we have taken $\lambda = 0.5$ and $y = 0.6$ at $\mu = 100$ GeV, and the non-local scale to be $M = 10^5$ GeV. As we expect, the scalar self-coupling stops its evolution around $\mu = M = 10^5$ GeV, while the running coupling in the standard theory becomes negative by the negative contribution form f_y.

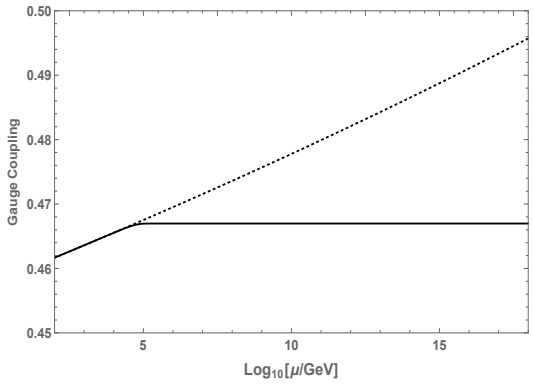

Figure 2.2: The running U(1) gauge coupling shown in solid (dashed) black lines for the non-local (local) theories. Here, we have taken $M = 10^5$ GeV.

2.3 Non-local QED

Next we study the gauge coupling running in the non-local QED. The incorporation of a gauge interaction is much the same as in the local QED case. Now due to the non-local nature of the theory the field strength is modified along with the covariant derivative expression. Consider the following gauge invariant Lagrangian for the non-local QED with a Dirac fermion [26],

$$\mathcal{L} = -\frac{1}{4} F^{\mu\nu} e^{\frac{\Box}{M^2}} F_{\mu\nu} + i\bar{\psi} e^{\frac{\nabla^2}{M^2}} \gamma^\mu D_\mu \psi + \text{H.c.}, \tag{2.14}$$

where $D_\mu = \partial_\mu + igA_\mu$ is the covariant derivative and $\nabla^2 = D_\mu D^\mu$. The covariant form in the exponential found in the fermion term is necessary, along with the hermitian conjugate of it, to ensure hermiticity of the Lagrangian.

Although Abelian gauge theories are asymptotically non-free in the standard QFT, their non-local extension results in a very interesting behavior. As in the standard QFT, we extract the β-function of the gauge coupling from the anomalous dimension of the gauge field as $\beta_g = \gamma_A$, which is calculated in Appendix C.

As mentioned previously, calculations of any wave function renormalizations is complicated. Borrowing our approach in determining the $f_{\lambda y}$ term above and assuming $\mu^2 \gg p_E^2$, we obtain the following expression for the RG equation of the gauge coupling (see

Appendix C):

$$\mu \frac{dg}{d\mu} = \frac{1}{16\pi^2} \left(\frac{4}{3}\right) g^3 e^{-2\frac{\mu^2}{M^2}}. \tag{2.15}$$

Clearly, the standard result retains in the limit of $M \to \infty$. Similarly to the RG evolutions of the scalar self-coupling and the Yukawa coupling, the influence of the non-local effects has essentially rendered a would-be asymptotic non-free theory UV finite or "UV-insensitive". From Eq. (2.15), it is evident that once the running of the couplings passes beyond the non-local scale M, the β-function rapidly approaches zero, resulting in a constant value of coupling as seen in Figure 2.2.

The advantage of a Gaussian kinetic operator is that the Abelian Higgs becomes scale free beyond energy scale, M. The theory becomes conformal, and M signifies the UV-fixed point. Conformal theory has many classical and quantum virtues, although the theory becomes trivial beyond M here, it is pertinent to think about how to generate the value of M. At this point, we merely speculate this scale beyond the SM and Planck scale, but its origin might arise from the scale of compactification from higher dimensions, or from the VEV of the dilaton, for instance in string theory [23, 24].

2.4 Applications to cosmology

One particular application for the scale free theory comes in the context of cosmological inflation, for a review see [54]. In this respect the value of M will play a significant role for breaking the scale invariance, as well as creating the density fluctuations observed in the cosmic microwave background radiation [55].

The freezing of the self-interaction term in the UV leads to a scale free potential beyond the energy scale of M. The field ϕ would be the ideal candidate for inflaton driving potential dominated inflation, since the fermion coupling also freezes, the radiative correction to ϕ from fermion-loop will not spoil the flatness of the potential all the way

beyond $M < M_p \simeq 2.4 \times 10^{18}$ GeV, and even beyond M_p. The potential maintains a perfect shift-symmetry, therefore ϕ can take any VEVs. In this respect realising super-Planckian VEV during inflation will not be forbidden, albeit there are quantum gravity corrections which are expected to be tiny, as long as the energy density of the inflationary vacuum is still below the Planckian energy density.

In the simplest scenario with $\lambda\phi^4$ potential the inflationary predictions are already ruled out by the current data from Planck [55], nevertheless a slight modification in the setup such as the SM Higgs inflation [56], might be a simple way to realize a falsifiable model of inflation. Indeed, the scale of non-locality will play a significant role here, which we will explore in future studies. Nevertheless, we can make some intriguing comments here already. Typically, in this setup we would require minimal kinetic term for Higgs, which is coupled to the Ricci scalar via a non-minimal coupling. In order to explain the amplitude of the observed density perturbations in the cosmic microwave background radiation (CMBR), we would expect the non-mininal coupling to be large of the order of $\mathcal{O}(4000)$, in order to sufficiently flatten the potential [56]. In our case, though, this non-minimal coupling can be made even order $\mathcal{O}(1)$, the flattening of the potential will essentially comes from the scale free theory, and the end of inflation will arise from the RG equation, which modifies the potential close to the scale of non-locality M. Indeed, all the details have to be worked out carefully to show that this mechanism can work properly for a viable model of inflation.

A point to contemplate in this regard is that besides the initial conditions which are to be chosen in order to evolve the differential equations to a point where the observables are measured or the Universe behave as it does today, we have introduced a degree of freedom (at least from mathematical point of view) choosing which suitably may give us the correct Universe even with starting off from an initial condition otherwise considered incompatible.

There is another intriguing feature for thermal history of the Universe. Since, all the

interactions freeze above M, the scattering rate, Γ, between species, i.e. scalar, fermion and Abelian gauge field, will not be able to cope with the Hubble expansion rate, H, of the Universe, i.e. $\Gamma \ll H$. Indeed, the expansion rate of the Universe would still be dominated by the dynamics of the scalar field, however, the Universe would be effectively *cold* for energy scale $\geq M$. The value of M would effectively determine the dynamics of reheating of the Universe, once the *big-freeze* in the interactions cease. This limits the reheat temperature of the Universe $T_{rh} \leq M$ for all practical purposes.

2.5 Conclusions

We have shown that within the Abelian Higgs model, a Gaussian kinetic operator, which introduces no new poles other than the original theory gives rise to a scale-invariant or a conformal theory in the UV beyond the scale of non-locality. The presence of non-locality arises in the interactions when the vertex operators gain exponential factors in the momentum space, smearing out the vertices. Infinite derivatives are required precisely to make the theory *ghost free* all the way from IR to UV. In this regard what we have shown is that the beta functions for the Abelian Higgs and the fermion exponentially decreases in the UV beyond the scale of non-locality, essentially making the theory dynamically stable beyond M. Indeed, the choice of M here is arbitrary. However, it is indicative that in the non-Abelian Higgs, such a new scale if appears around $10^{10} - 10^{11}$ GeV would definitely yield a stable SM Higgs without invoking any new symmetries. Our results open a new way to model the stability issue concerning any scalar field theory, a detailed RG equations of non-Abelian Higgs will be presented in a separate publication.

Finally, we wish to make a comment on introducing non-locality for the non-Abelian Higgs and SM fermions. Despite the $SU(2)_L$ structure making the loop computations a bit more complicated, the final outcomes are very similar to that of the Abelian Higgs in presence of non-locality. The Gaussian kinetic term will always pave the exponential suppression in the propagator in the UV, while enhancing the vertex operators. It is easy

to show that the self-interacting non-local terms from the non-Abelian generators (arising due to covariant derivatives) only contribute as higher and higher dimensional operators thus highly suppressed by powers of M. The UV behaviour of the Higgs will be very similar to what we have discussed in the Abelian case, including the leading order behaviour of the beta-functions for the SM Higgs and the fermions.

2.A Appendix for Wave Function Renormalization

Our methodology for calculating the wave function renormalization follows from the same procedure of calculating quantum corrections in conventional quantum field theories. As all quantum corrections are switched off at energies beyond scale M in non-local theories, strictly speaking there are no corrections in this UV regime. However, our guiding philosophy is that as the non-local scale is pushed towards the limit of $M \to \infty$, we need to recover all the results in the conventional quantum field theories.

2.A.1 Scalar Wave Function Renormalization

The 2-point 1-PI function in Eq. (2.6) is explicitly given by

$$\begin{aligned}
\Gamma_2 &= y^2 \int \frac{d^4k_E}{(2\pi)^4} \,\mathrm{tr}\left[\Pi_\psi(k_E)\,\Pi_\psi(k_E+p_E)\right] \\
&= y^2 \int \frac{d^4k_E}{(2\pi)^4} \,\mathrm{tr}\left[\Pi_\psi(k_E-p_E/2)\,\Pi_\psi(k_E+p_E/2)\right] \\
&= 4y^2 \int \frac{d^4k_E}{(2\pi)^4} \frac{(k_E-\frac{p_E}{2})\cdot(k_E+\frac{p_E}{2})}{(k_E-\frac{p_E}{2})^2(k_E+\frac{p_E}{2})^2}\, e^{-\beta(k_E-\frac{p_E}{2})^2} e^{-\beta(k_E+\frac{p_E}{2})^2},
\end{aligned} \tag{2.16}$$

where $\beta = 1/M^2$. Using the Schwinger parameters, α_1 and α_2, and completing the square in the exponent yields

$$\begin{aligned}
\Gamma_2 &= 4y^2 \int \frac{dk_E^4}{(2\pi)^4} \int_0^\infty d\alpha_1 d\alpha_2 \left(k_E-\frac{p_E}{2}\right)\cdot\left(k_E+\frac{p_E}{2}\right) \\
&\quad \times e^{-\left((\alpha_1+\alpha_2+2\beta)^{1/2}k_E+\frac{\alpha_1-\alpha_2}{(\alpha_1+\alpha_2+2\beta)^{1/2}}\frac{p_E}{2}\right)^2} e^{-\left(\alpha_1+\alpha_2+2\beta-\left(\frac{\alpha_1-\alpha_2}{(\alpha_1+\alpha_2+2\beta)^{1/2}}\right)^2\right)\frac{p_E^2}{4}}.
\end{aligned} \tag{2.17}$$

Introducing new parameters defined as $\alpha_1 + \alpha_2 = s$ and $\alpha = \alpha_1/s$, and shifting the momentum by $k_E \to k_E - \frac{s(2\alpha-1)}{s+2\beta}\frac{p_E}{2}$, we express Γ_2 as

$$\begin{aligned}\Gamma_2 &= 4y^2 \int \frac{dk_E^4}{(2\pi)^4} \int_0^1 d\alpha \int_0^\infty sds \left(k_E^2 - \left[1 - \left(\frac{s(2\alpha-1)}{(s+2\beta)} \right)^2 \right] \frac{p_E^2}{4} \right) \\ &\quad \times e^{-\left((s+2\beta)k_E^2 + \left(s+2\beta - \left(\frac{s(2\alpha-1)}{(s+2\beta)^{1/2}} \right)^2 \right) \frac{p_E^2}{4} \right)}. \end{aligned} \tag{2.18}$$

We extract the wave function renormalization factor as a coefficient of the external momentum $(-p_E^2)$ by

$$\begin{aligned}&\frac{\partial}{\partial(-p_E^2)} \Gamma_2 \Big|_{p_E^2=0} = \frac{y^2}{16\pi^2} \int^{\Lambda^2} k_E^2 dk_E^2 \int_0^1 d\alpha \int_0^\infty sds\, e^{-(s+2\beta)k_E^2} \\ &\times \left(k_E^2 \left[s + 2\beta - \left(\frac{s(2\alpha-1)}{(s+2\beta)^{1/2}} \right)^2 \right] + 1 - \left[\frac{s(2\alpha-1)}{s+2\beta} \right]^2 \right) \\ &\approx \frac{y^2}{16\pi^2} \int^{\Lambda^2} k_E^2 dk_E^2 \left(\frac{3 + 2\beta k_E^2}{k_E^4} - \frac{1}{3} \left[\frac{2 - 2\beta k_E^2 + 4\beta^2 k_E^4}{k_E^4} + \frac{1 - 4\beta k_E^2 - 4\beta^2 k_E^4}{k_E^4} \right] \right) e^{-2\beta k_E^2} \\ &= \frac{2y^2}{16\pi^2} \int^{\Lambda^2} dk_E^2 \frac{e^{-2\beta k_E^2}}{k_E^2}. \end{aligned} \tag{2.19}$$

Here, the approximation indicates that terms which rapidly approach zero for $k_E^2 > M^2$ are excluded for simplicity. Applying the standard QFT procedure, we obtain the anomalous dimension as

$$\gamma_\phi = \frac{1}{2}\Lambda \frac{\partial}{\partial \Lambda} \left[\frac{\partial}{\partial(-p_E^2)} \Gamma_2 \Big|_{p_E^2=0} \right] \Big|_{\Lambda \to \mu} = \frac{y^2}{8\pi^2} e^{-2\beta\mu^2}. \tag{2.20}$$

2.A.2 Fermion Wave Function Renormalization

Employing similar techniques and Schwinger parameterizations as outlined for the scalar field, we calculate the fermion wave function renormalization. The 1-loop calculation

is given by

$$\begin{aligned}
\Gamma_2 &= -y^2 \int \frac{d^4k_E}{(2\pi)^4} \Pi_\psi(k_E + p_E/2)\, \Pi_\phi(k_E - p_E/2) \\
&= -y^2 \int \frac{d^4k_E}{(2\pi)^4} \frac{\not{k}_E + \frac{\not{p}_E}{2}}{(k_E - \frac{p_E}{2})^2 (k_E + \frac{p_E}{2})^2} e^{-\beta(k_E - \frac{p_E}{2})^2} e^{-\beta(k_E + \frac{p_E}{2})^2} \qquad (2.21) \\
&= -y^2 \int \frac{d^4k_E}{(2\pi)^4} \int d\alpha_1 d\alpha_2 \left(\not{k}_E + \frac{\not{p}_E}{2} \right) \\
&\quad \times e^{-\left((\alpha_1+\alpha_2+2\beta)^{1/2} k + \frac{\alpha_1-\alpha_2}{(\alpha_1+\alpha_2+2\beta)^{1/2}} \frac{p_E}{2} \right)^2} e^{-\left(\alpha_1+\alpha_2+2\beta - \left(\frac{\alpha_1-\alpha_2}{(\alpha_1+\alpha_2+2\beta)^{1/2}} \right)^2 \right) \frac{p_E^2}{4}}. \qquad (2.22)
\end{aligned}$$

As in the scalar case, redefining the Schwinger parameters and shifting the momentum, we express

$$\begin{aligned}
\Gamma_2 &= -y^2 \int \frac{d^4k_E}{(2\pi)^4} \int_0^1 d\alpha \int_0^\infty s ds \left(\not{k}_E + \left[1 - \frac{s(2\alpha-1)}{s+2\beta} \right] \frac{\not{p}_E}{2} \right) \qquad (2.23) \\
&\times \; e^{-\left((s+2\beta) k_E^2 + \left(s+2\beta - \left(\frac{s(2\alpha-1)}{(s+2\beta)^{1/2}} \right)^2 \right) \frac{p_E^2}{4} \right)}.
\end{aligned}$$

We now extract the wave function renormalization factor as a coefficient of the external momentum $\not{p}_E$ by

$$\begin{aligned}
\frac{\partial}{\partial \not{p}_E} \Gamma_2 \Big|_{p_E=0} &= \frac{y^2}{16\pi^2} \left(\frac{1}{2} \right) \int^{\Lambda^2} k_E^2 dk_E^2 \int_0^1 d\alpha \int_0^\infty s ds \\
&\quad \times \left(1 - \frac{s(2\alpha-1)}{s+2\beta} \right) e^{-(s+2\beta)k_E^2} \\
&= \frac{y^2}{16\pi^2} \left(\frac{1}{2} \right) \int^{\Lambda^2} dk_E^2 \, \frac{e^{-2\beta k_E^2}}{k_E^2}. \qquad (2.24)
\end{aligned}$$

Hence, we obtain the anomalous dimension for the fermion as

$$\gamma_\psi = \frac{1}{2} \Lambda \frac{\partial}{\partial \Lambda} \left[\frac{\partial}{\partial \not{p}_E} \Gamma_2 \Big|_{p_E=0} \right] \Big|_{\Lambda \to \mu} = \frac{y^2}{32\pi^2} e^{-2\beta\mu^2}. \qquad (2.25)$$

2.A.3 Gauge Wave Function Renormalization

The β-function in Eq. (2.15) originates from the fermion loop contribution to the wave function renormalization of the gauge field. Employing the similar techniques in Appendices A and B, we express the 2-point 1-PI function of the gauge field as

$$\begin{aligned}\Gamma_2 &= g^2 \int \frac{d^4k_E}{(2\pi)^4} \int_0^1 d\alpha \int_0^\infty sds \ (g_{\rho\nu}g_{\sigma\mu} - g_{\mu\nu}g_{\rho\sigma} + g_{\rho\mu}g_{\sigma\nu}) \\ &\times \left(k_E - \left[1 + \frac{s(2\alpha-1)}{s+2\beta}\right]\frac{p_E}{2}\right)^\rho \left(k_E + \left[1 - \frac{s(2\alpha-1)}{s+2\beta}\right]\frac{p_E}{2}\right)^\sigma \\ &\times e^{-\left((s+2\beta)k_E^2 + \left(s+2\beta - \left(\frac{s(2\alpha-1)}{(s+2\beta)^{1/2}}\right)^2\right)\frac{p_E^2}{4}\right)}. \end{aligned} \tag{2.26}$$

Dropping all terms odd in loop momentum, and using $\int d^4k k^\mu k^\nu f(k^2) = \frac{1}{4}\int d^4k k^2 g^{\mu\nu} f(k^2)$, we simplify the 2-point function as

$$\begin{aligned}\Gamma_2 &= \frac{g^2}{16\pi^2} \int^{\Lambda^2} k_E^2 dk_E^2 \int_0^1 d\alpha \int_0^\infty sds \\ &\times \left(-2k_E^2 g_{\mu\nu} - 4\left[1 - \left(\frac{s(2\alpha-1)}{s+2\beta}\right)^2\right]\left[\frac{p_{E\mu}p_{E\nu}}{2} - \frac{p_E^2 g_{\mu\nu}}{4}\right]\right) \\ &\times e^{-\left((s+2\beta)k_E^2 + \left(s+2\beta - \left(\frac{s(2\alpha-1)}{(s+2\beta)^{1/2}}\right)^2\right)\frac{p_E^2}{4}\right)}. \end{aligned} \tag{2.27}$$

To easily find the wave function renormalization, we focus on the coefficient of terms only proportional to $p_{E\mu}p_{E\nu}$, which gives

$$\begin{aligned}\Gamma_2 &\supset -\frac{2g^2}{16\pi^2}(p_{E\mu}p_{E\nu}) \int^{\Lambda^2} k_E^2 dk_E^2 \int_0^1 d\alpha \int_0^\infty sds \left(1 - \frac{s^2(2\alpha-1)^2}{(s+2\beta)^2}\right) e^{-(s+2\beta)k_E^2} \\ &\approx -\frac{g^2}{8\pi^2}\left(\frac{4}{3}\right)(p_{E\mu}p_{E\nu}) \int^{\Lambda^2} dk_E^2 \frac{e^{-2\beta k_E^2}}{k_E^2} \end{aligned} \tag{2.28}$$

From this formula, we read off the β-function in Eq. (2.15).

CHAPTER 3

DOMAIN-WALL STANDARD MODEL IN NON-COMPACT 5D AND LHC PHENOMENOLOGY

3.1 Introduction

A possibility that our world consists of more than 4-dimensional space-time has been attracting a good deal of attention for a long time. After the discovery of the D-brane in string theories [57], the brane-world scenario has been intensively studied as new physics beyond the Standard Model (SM). In extra-dimensional theories, a new property, "geometry," comes into play in phenomenology and provides us with a new possibility of understanding mysteries within the SM. The large extra-dimension model [9] is a well-known brane-world scenario which offers a solution to the gauge hierarchy problem by "diluting" the Planck scale to the TeV scale by a large extra-dimensional volume. Another well-known scenario is the warped extra-dimension model [30], where the Planck scale is "warped down" to the TeV scale in the presence of the anti-de Sitter (AdS) curvature in the extra 5th dimension.

In most of the extra-dimensional models that have been investigated until now, extra-dimensions are assumed to be compactified on some manifolds or orbifolds, and they are treated differently from our 3-spatial dimensions. We may suppose it more natural if all spatial dimensions are non-compact and the SM is realized as a 4-dimensional effective theory. This picture requires that all SM fields as well as 4-dimensional graviton are localized in certain 3-spatial dimensional domains in the bulk space. A simple realization of this picture for 4-dimensional graviton has been proposed in Ref. [58], the so-called RS-2

scenario, where due to the 5-dimensional AdS curvature, 4-dimensional graviton is localized at a point in non-compact 5th dimension and the Einstein gravity in 4 dimensions is reproduced at low energies.

In this chapter, we propose a framework to construct "Domain-Wall Standard Model" in 5-dimensional space-time, where all the SM fields, including the gauge bosons, are localized in certain domains along the 5th dimension. This direction has been considered in Ref. [35] before, where the SU(5) gauge symmetry is introduced in the 5-dimensional bulk and the Dvali-Shifman mechanism [36] is assumed for dynamically localizing the SM gauge bosons associated with the breaking of the SU(5) gauge symmetry down to the SM gauge group. In this chapter, we consider a simple way for localizing a gauge field in the bulk without extending the SM gauge groups, which has been proposed in Ref. [37]. We utilize the same mechanism for the localization of the SM Higgs field, while the SM fermions are localized via the mechanism proposed in Ref. [38] (domain-wall fermion). Our scenario is a field-theoretical realization of a "3-brane" in which all the SM fields are confined. However, the finite width of the "3-brane" leads to rich physics phenomenologies that can be explored in future Large Hadron Collider (LHC) experiments.

In the next section, we describe the basic construction of the Domain-Wall SM, where all the SM fields (the gauge bosons, the Higgs field, and the chiral fermions) are localized via certain mechanisms. Effective couplings between Kaluza-Klein (KK) modes of the SM gauge bosons and the SM fermions are derived in the 4-dimensional effective theory. We discuss the collider phenomenology on KK-modes of the SM gauge bosons in Sec. 3.3. The current results from the search for a new gauge boson resonance at the LHC Run-2 is interpreted as constraints on our model. In the last section, we summarize our results and discuss future directions for the Domain-Wall SM.

3.2 Basic construction of Domain-Wall Standard Model

In realizing the Domain-Wall SM, we need localization mechanisms for the myriad of SM fields: the gauge fields, the Higgs field, and the chiral fermions. In this section, we present the basics construction of the Domain-Wall SM.

3.2.1 Gauge field localization

Since the essence for localizing a gauge field is independent of the gauge structure, we address the gauge field localization based on a U(1) gauge theory. A simple way of localizing the gauge field has been proposed in Ref. [37], where a gauge coupling depending on the 5th coordinate is introduced.[1] In 5-dimensional flat Minkowski space-time, the basic Lagrangian for the U(1) gauge field is of the form,

$$\mathcal{L}_5 = -\frac{1}{4} s(y) F_{MN} F^{MN}, \tag{3.1}$$

where F_{MN} is the gauge field strength, and $M, N = 0, 1, 2, 3, y$ with y being the index for the 5th extra-dimensional coordinate. Our convention for the metric is $\eta_{MN} = \mathrm{diag}(1, -1, -1, -1, -1)$, and in general we suppress coordinate dependence of the fields unless emphasis is needed. Note that the gauge coupling $1/g^2 = s(y)$ depends on the 5th coordinate y. Decomposing the field strength into its components yields the following expression (up to total derivative terms):

$$\begin{aligned} \mathcal{L}_5 &= \frac{1}{2} s A^\mu \left(g_{\mu\nu} \Box_4 - \partial_\mu \partial_\nu \right) A^\nu - \frac{1}{2} s A_y \Box_4 A_y \\ &- \frac{1}{2} A_\mu \partial_y \left(s \partial_y A^\mu \right) - \left(\partial_\mu A^\mu \right) \partial_y \left(s A_y \right), \end{aligned} \tag{3.2}$$

where A_μ ($\mu = 0, 1, 2, 3$) and A_y are a gauge field and a scalar field in 4-dimensional space-time, and the first line in the right-hand-side denotes the 4-dimensional kinetic terms

[1] The same idea was discussed elsewhere before Ref. [37]. See, for example, Ref. [59]

for these fields.[2] The last term contains a mixing between A_μ and A_y. Note that this structure is analogous to that in spontaneously broken gauge theories, and we eliminate the mixing term by adding a gauge fixing term, which is a 5-dimensional analog to the R_ξ gauge:[3]

$$\mathcal{L}_{\rm GF} = -\frac{s}{2\,\xi}\left(\partial_\mu A^\mu - \frac{\xi}{s}\partial_y(sA_y)\right)^2, \tag{3.3}$$

where ξ is a constant parameter. The total Lagrangian now reads
$\mathcal{L} = \mathcal{L}_5 + \mathcal{L}_{\rm GF} = \mathcal{L}_{gauge} + \mathcal{L}_{scalar}$, where

$$\mathcal{L}_{gauge} = \frac{1}{2}sA^\mu\left(g_{\mu\nu}\Box_4 - \left(1-\frac{1}{\xi}\right)\partial_\mu\partial_\nu\right)A^\nu - \frac{1}{2}A_\mu\partial_y(s\,\partial_y A^\mu), \tag{3.4}$$

$$\mathcal{L}_{scalar} = -\frac{1}{2}sA_y\Box_4 A_y + \frac{1}{2}s\,\xi A_y\partial_y\left(\frac{1}{s}\partial_y(sA_y)\right). \tag{3.5}$$

Next, we analyze the Kaluza-Klein (KK) modes of the gauge and scalar fields via the mode expansions

$$A_\mu(x,y) = \sum_{n=0}^{\infty} A_\mu^{(n)}(x)\chi^{(n)}(y), \quad A_y(x,y) = \sum_{n=0}^{\infty}\eta^{(n)}(x)\psi^{(n)}(y), \tag{3.6}$$

where $x = x^\mu$. From Eqs. (3.4) and (3.5), we obtain the KK-mode equations:

$$\frac{d}{dy}\left(s\,\frac{d}{dy}\chi^{(n)}\right) + s\,m_n^2\chi^{(n)} = 0, \quad \frac{d}{dy}\left(\frac{1}{s}\frac{d}{dy}(s\psi^{(n)})\right) + \tilde{m}_n^2\psi^{(n)} = 0. \tag{3.7}$$

With the solutions of these KK-mode equations, the Lagrangians in Eqs. (3.4) and (3.5)

[2] In literature, authors sometimes employ the "axial gauge" $A_y = 0$ to simplify the 5-dimensional equations of motion for the gauge field. However, this procedure may be misleading, since as we will see in the following, the zero-mode of A_y vanishes not by the gauge-fixing but due to the explicit breaking of the 5-dimensional gauge invariance by $s(y)$. This is analogous to the 5-dimensional models with a S_1/Z_2 orbifold compactification, where A_y for the zero-mode is projected out by the orbifolding, but not by the axial gauge-fixing. In our discussion, the gauge transformation is employed to eliminate 2 degrees of freedom from A_μ as usual in 4-dimensional gauge field theories, and A_y is left as a dynamical field.

[3] During the completion of our manuscript, we have learned that another group is considering a more general procedure for localized gauge fields [60].

are written as

$$\begin{aligned}
\mathcal{L}_{gauge} &= \sum_{n=0}^{\infty} \frac{1}{2} s \left(\chi^{(n)}\right)^2 \left[A_\mu^{(n)} \left(g^{\mu\nu} (\Box_4 + m_n^2) - \left(1 - \frac{1}{\xi}\right) \partial^\mu \partial^\nu \right) A_\nu^{(n)} \right], \\
\mathcal{L}_{scalar} &= -\sum_{n=0}^{\infty} \frac{1}{2} s \left(\psi^{(n)}\right)^2 \left[\eta^{(n)} \left(\Box_4 + \xi\, \tilde{m}_n^2 \right) \eta^{(n)} \right],
\end{aligned} \tag{3.8}$$

Note that if the two equations in Eq. (3.7) have solutions with $m_n = \tilde{m}_n$, Eq. (3.8) indicates that the relation between $A_\mu^{(n)}$ and $\eta^{(n)}$ in the 4-dimensional effective theory is nothing but the one between a massive gauge boson and a would-be Nambu-Goldstone (NG) mode in the R_ξ gauge after the spontaneous gauge symmetry breaking. In this case, we can identify the KK-modes of $\eta^{(n)}$ with would-be NG modes eaten by the KK-modes of $A_\mu^{(n)}$. From the view point of 4-dimensional effective theory, this picture seems quite reasonable. In fact, we find $m_n = \tilde{m}_n$ for the solvable example that we discuss in the following.

Even for a general function of $s(y)$, it is easy to find zero-mode solutions with $m_0 = 0$ in Eq. (3.7). General solutions are given by

$$\chi^{(0)} = \tilde{c}_\chi + c_\chi \int^y dy' \frac{1}{s(y')}, \quad \psi^{(0)} = \frac{\tilde{c}_\psi}{s(y)} + \frac{c_\psi}{s(y)} \int^y dy' s(y'), \tag{3.9}$$

where $\tilde{c}_\chi$, c_χ, $\tilde{c}_\psi$, and c_ψ are constants. In order to localize the gauge field in the finite domain, we impose $s(y) \to 0$ as $|y| \to \infty$. In addition, the gauge field in the 4-dimensional effective theory must be normalizable in the sense that

$$\int_{-\infty}^{\infty} dy\, s(y)\, \chi^{(n)}(y)\, \chi^{(n)}(y) < \infty. \tag{3.10}$$

Considering the zero-mode solution for the gauge field, this constraint requires $c_\chi = 0$, resulting in the zero-mode for the gauge boson having a constant configuration in the 5th coordinate direction. Note that this forces the gauge coupling to be universal in the 4-dimensional effective theory and hence the 4-dimensional gauge invariance is maintained.

Applying the same logic to the scalar A_y component yields an interesting result: the solution of $\psi^{(0)}$ cannot satisfy the requirement given in Eq. (3.10) unless $c_\psi = \tilde{c}_\psi = 0$. This suggests to us that $\psi^{(0)} = 0$ is the only appropriate choice for the zero-mode of the scalar. Hence, no (normalizable) zero-mode exists for the scalar component. Note that if $s(y)$ is independent of y, a constant $\psi^{(0)}$ becomes a consistent solution. This is a trivial case where the 5-dimensional gauge invariance is manifest. Therefore, the absence of the zero-mode scalar originates from the explicit breaking of the 5-dimensional gauge invariance due to y-dependence of the gauge coupling $s(y)$.

For the following discussion about the LHC phenomenology, let us consider a solvable example for $s(y)$ as

$$s(y) = \begin{cases} S_0 + \epsilon & (|y| < L) \\ \epsilon & (|y| > L) \end{cases} = S_0 \left[H(y+L) - H(y-L) \right] + \epsilon, \tag{3.11}$$

where S_0 and ϵ are real, positive constants, $H(x)$ is the Heaviside function, and we have introduced the small parameter $\epsilon \ll S_0$ to regularize $1/s(y)$. Since $s(y)$ is invariant under the reflection of the 5th coordinate $y \to -y$, let us simplify our system by introducing Z_2-parity. Under $y \to -y$, the Lagrangian in Eq. (3.2), and A_μ are even, while A_y is odd. Now we can easily find the solution to the KK-mode equations in Eq. (3.7) for $y \neq \pm L$ and the KK-mode expansions are expressed as

$$A_\mu(x,y) = A_\mu^{(0)}(x) + \sum_{n=1}^{\infty} A_\mu^{(n)}(x) \cos(m_n y), \quad A_y(x,y) = \sum_{n=1}^{\infty} \eta^{(n)}(x) \sin(m_n y). \tag{3.12}$$

Although the zero-mode of A_y is projected out because of the Z_2-parity in the present system, the zero-mode doesn't exist in any cases as we have discussed above. Since $ds(y)/dy$ is singular at $y = \pm L$, boundary conditions are imposed to make the solutions

regular, namely,

$$\frac{d}{dy}A_\mu(x,y)\,|_{y\to\pm L}=0,\quad A_y(x,y)\,|_{y\to\pm L}=0. \tag{3.13}$$

Thus we find the mass eigenvalue for each KK-mode of $A_\mu^{(n)}$ as $m_n = n(\pi/L)$, while the mass for each KK-mode of $\eta^{(n)}$, which is a would-be NG mode eaten by the corresponding $A_\mu^{(n)}$, is given by ξm_n^2. By integrating out the 5th-dimensional degrees of freedom and taking a limit $\epsilon \to 0$, the 4-dimensional effective Lagrangian is then

$$\begin{aligned}
\mathcal{L}_4 &= \int_{-\infty}^{\infty} dy\,\mathcal{L}_5 \\
&= \frac{1}{2}\left(\frac{1}{g}\right)^2 A_\mu^{(0)}\left[g^{\mu\nu}\Box_4-\left(1-\frac{1}{\xi}\right)\partial^\mu\partial^\nu\right]A_\nu^{(0)} \\
&+ \frac{1}{2}\left(\frac{1}{\sqrt{2}\,g}\right)^2\sum_{n=1}^{\infty}\left\{A_\mu^{(n)}\left[g^{\mu\nu}\left(\Box_4+m_n^2\right)-\left(1-\frac{1}{\xi}\right)\partial^\mu\partial^\nu\right]A_\nu^{(n)}\right\} \\
&- \frac{1}{2}\left(\frac{1}{\sqrt{2}\,g}\right)^2\sum_{n=1}^{\infty}\left[\eta^{(n)}\left(\Box_4+\xi m_n^2\right)\eta^{(n)}\right],
\end{aligned} \tag{3.14}$$

where we have defined the gauge coupling (g) in the 4-dimensional effective theory as $1/g^2 = 2S_0L$. Note that this effective Lagrangian is the same as the one obtained from a 5-dimensional gauge theory by compactifying the 5th dimension on S^1/Z_2 orbifold with a radius L/π, (see, for example, Ref. [61]). For this solvable example, we have obtained an effectively compactified 5-dimensional gauge theory. However, as we will see in the following, the KK-model phenomenology is quite different, since the SM fermions have non-trivial configurations in the 5th dimension.

3.2.2 Localized Higgs field

Next we consider the 5-dimensional extension of the Higgs mechanism. To simplify our discussion, we take the Abelian Higgs model as an example, corresponding to our previous discussion about the localized U(1) gauge field. It is straightforward to extend our discussion to the SM Higgs doublet case.

In non-compact extra-dimensions, we need to consider a localization mechanism for not only Higgs field but also its vacuum expectation value. For this purpose, we may utilize the same procedure taken for the gauge field, and the Lagrangian for the Higgs sector is defined as

$$\mathcal{L}_5^H = s(y)\left[(\mathcal{D}^M H)^\dagger(\mathcal{D}_M H) - \frac{1}{2}\lambda\left(H^\dagger H - \frac{v^2}{2}\right)^2\right], \tag{3.15}$$

where H is the Higgs field, λ is a Higgs quartic coupling, v is its vacuum expectation value, and the covariant derivative is given by $\mathcal{D}_M = \partial_M - iQ_H A_M$ with a U(1) charge Q_H for the Higgs field. Here, we define the Higgs field as a Z_2-even field with a mass dimension 1.

Expanding about the vacuum $H = (v + h + i\phi)/\sqrt{2}$ and neglecting the interaction terms, we obtain (up to total derivative terms)

$$\begin{aligned}\mathcal{L}_5^H &\supset \frac{1}{2}s(y)\left[(\partial^M h)(\partial_M h) - m_h^2 h^2\right] + \frac{1}{2}s(y)(\partial^M\phi)(\partial_M\phi) \\ &= -\frac{1}{2}sh(\Box_4 + m_h^2)h + \frac{1}{2}h\,\partial_y(s\partial_y h) - \frac{1}{2}s\phi\Box_4\phi + \frac{1}{2}\phi\,\partial_y(s\partial_y\phi),\end{aligned} \tag{3.16}$$

where $m_h^2 = \lambda v^2$ is the physical Higgs boson mass. From the KK-mode decomposition for these fields,

$$h(x,y) = \sum_{n=0}^{\infty} h^{(n)}(x)\chi_h^{(n)}(y), \quad \phi(x,y) = \sum_{n=0}^{\infty}\phi^{(n)}(x)\chi_\phi^{(n)}(y), \tag{3.17}$$

we can see that the KK-mode equations for $\chi_h^{(n)}$ and $\chi_\phi^{(n)}$ are identical to that of the gauge boson in Eq. (3.7). Since the zero-mode $\phi^{(0)}$ is the would-be NG mode eaten by $A_\mu^{(0)}$, the theoretical consistency requires the configurations of $\phi^{(0)}$ and $A_\mu^{(0)}$ to be identical. With the same eigenfunctions as the gauge bosons, the free Lagrangian for the scalar fields are given

by

$$\mathcal{L}_4^H \supset -\frac{1}{2}\left(\frac{1}{g}\right)^2 h^{(0)}\left(\Box_4 + m_h^2\right) h^{(0)} - \frac{1}{2}\left(\frac{1}{\sqrt{2}\,g}\right)^2 \sum_{n=1}^{\infty}\left[h^{(n)}\left(\Box_4 + \left(m_h^2 + m_n^2\right)\right) h^{(n)}\right] + \left\{h^{(m)} \to \phi^{(m)},\ m_h \to 0\right\} \tag{3.18}$$

The U(1) gauge symmetry is broken by $\langle H\rangle = v/\sqrt{2}$, and the U(1) gauge boson acquires its mass. After normalizing the kinetic terms for all zero-modes and KK-modes, we find the gauge boson masses,

$$m_A^{(0)} = Q_H g v_h, \quad m_A^{(n)} = \sqrt{m_n^2 + (Q_H g v_h)^2}, \tag{3.19}$$

for the zero-mode and the KK-modes, respectively. Here we have defined v_h as $v_h = v/g$ by considering the normalizations.

3.2.3 Domain-wall fermions

Next is the consideration of 5-dimensional fermions. Here we also consider the U(1) gauge theory to simply our discussion, which can be easily extended to the 5-dimensional SM case. We follow a mechanism in Ref. [38] to generate the domain-wall fermion in 5-dimensional space-time.

Let us first consider a real scalar field ($\varphi(x, y)$) in the 5-dimensional bulk:

$$\mathcal{L}_{(5)} = \frac{1}{2}\left(\partial_M \varphi\right)\left(\partial^M \varphi\right) - V(\varphi)\ , \tag{3.20}$$

where the scalar potential is give by

$$V(\varphi) = \frac{m_\varphi^4}{2\lambda} - m_\varphi^2 \varphi^2 + \frac{\lambda}{2}\varphi^4. \tag{3.21}$$

We may assign Z_2-odd parity for φ. This parity assignment is consistent with having a

non-trivial solution to the equation of motion, namely, the so-called kink solution,

$$\varphi_0(y) = \frac{m_\varphi}{\sqrt{\lambda}} \tanh[m_\varphi y]. \tag{3.22}$$

Following Ref. [38], we introduce the Lagrangian for a bulk fermion coupling with φ,

$$\begin{aligned} \mathcal{L} &= i\overline{\psi}\left[\gamma^\mu D_\mu + i\gamma^5 D_y\right]\psi + Y\varphi\overline{\psi}\psi \\ &= i\overline{\psi_L}\gamma^\mu D_\mu \psi_L + i\overline{\psi_R}\gamma^\mu D_\mu \psi_R \\ &- \overline{\psi_L} D_y \psi_R + \bar{\psi}_R D_y \psi_L + Y\varphi\left(\overline{\psi_L}\psi_R + \overline{\psi_R}\psi_L\right), \end{aligned} \tag{3.23}$$

where we decompose the Dirac fermion ψ into its chiral components, $\psi = \psi_L + \psi_R$, the covariant derivative is given by $D_M = \partial_M - iQ_f A_M$ with a U(1) charge Q_f for ψ, and Y is a positive constant. We define Z_2-parity for ψ_L and ψ_R to be even and odd, respectively. Neglecting the gauge interaction and replacing φ by the kink solution, the equations of motion are given by

$$\begin{aligned} i\gamma^\mu \partial_\mu \psi_L - \partial_y \psi_R + Y\varphi_0 \psi_R = 0, \\ i\gamma^\mu \partial_\mu \psi_R + \partial_y \psi_L + Y\varphi_0 \psi_L = 0. \end{aligned} \tag{3.24}$$

Since we are interested in the zero-mode solution that corresponds to a SM chiral fermion, we focus on the equations of motion for zero-modes: $\psi_L(x,y) \supset \psi_L^{(0)}(x)\,\chi_L^{(0)}(y)$ and $\psi_R(x,y) \supset \psi_R^{(0)}(x)\,\chi_R^{(0)}(y)$, such that[4]

$$\left(\frac{d}{dy} + Y\varphi_0\right)\chi_L^{(0)} = 0, \quad \left(\frac{d}{dy} - Y\varphi_0\right)\chi_R^{(0)} = 0. \tag{3.25}$$

[4]See Ref. [62] for complete analysis.

In the vicinity of $y = 0$, $\varphi_0 \simeq m_\varphi^2 y/\sqrt{\lambda}$, and we can find the approximate solutions as

$$\chi_L^{(0)} = C_L e^{-\frac{M_F^2}{2}y^2}, \quad \chi_R^{(0)} = C_R e^{+\frac{M_F^2}{2}y^2}, \tag{3.26}$$

where $C_{L,R}$ are constants, and $M_F = \sqrt{Y m_\varphi^2/\sqrt{\lambda}}$. Since χ_R is Z_2-odd, $C_R = 0$ and the right-handed chiral fermion is projected out.[5] Therefore, we have only one chiral fermion in the 4-dimensional effective theory. We fix $C_L = \sqrt{M_F/\sqrt{\pi}}$ and canonically normalize the fermion kinetic term.

Now we describe the Lagrangian for the chiral fermion in the 4-dimensional effective theory as

$$\begin{aligned} \mathcal{L}_4 \supset & \left[\int_{-\infty}^{\infty} dy \left(\chi_L^{(0)}\right)^2\right] \overline{\psi}_L^{(0)} i\gamma^\mu \left(\partial_\mu - iQ_f A_\mu^{(0)}\right) \psi_L^{(0)} \\ & + \sum_{n=1}^{\infty} Q_f \left[\int_{-\infty}^{\infty} dy \left(\chi_L^{(0)}\right)^2 \cos(m_n y)\right] A_\mu^{(n)} \left[\overline{\psi}_L^{(0)} \gamma^\mu \psi_L^{(0)}\right] \end{aligned} \tag{3.27}$$

Rescaling the gauge fields to canonically normalize their kinetic terms in Eq. (3.14), we obtain the final expression as

$$\mathcal{L}_4 \supset \overline{\psi}_L^{(0)} i\gamma^\mu \left(\partial_\mu - iQ_f g A_\mu^{(0)}\right) \psi_L^{(0)} + \sum_{n=1}^{\infty} Q_f g_{\rm eff}^{(n)} A_\mu^{(n)} \left[\overline{\psi}_L^{(0)} \gamma^\mu \psi_L^{(0)}\right], \tag{3.28}$$

where the 4-dimensional effective coupling between the chiral fermion and the KK-mode gauge boson is given by

$$g_{\rm eff}^{(n)} = \sqrt{2}\, g \, \exp\left[-\frac{1}{4}\left(\frac{m_n}{M_F}\right)^2\right]. \tag{3.29}$$

The widths of localized gauge fields and the chiral fermion are characterized by $1/m_n$ and $1/M_F$, respectively. A limit $M_F \to \infty$ corresponds to the case that the chiral fermion is localized on a "3-brane" with zero-width and all KK-modes of the bulk gauge boson

[5] Here, Z_2-parity is not essential. Even without introducing the Z_2-parity, the right-handed chiral fermion is delocalizing at $y = 0$ and thus it is not normalizable [38].

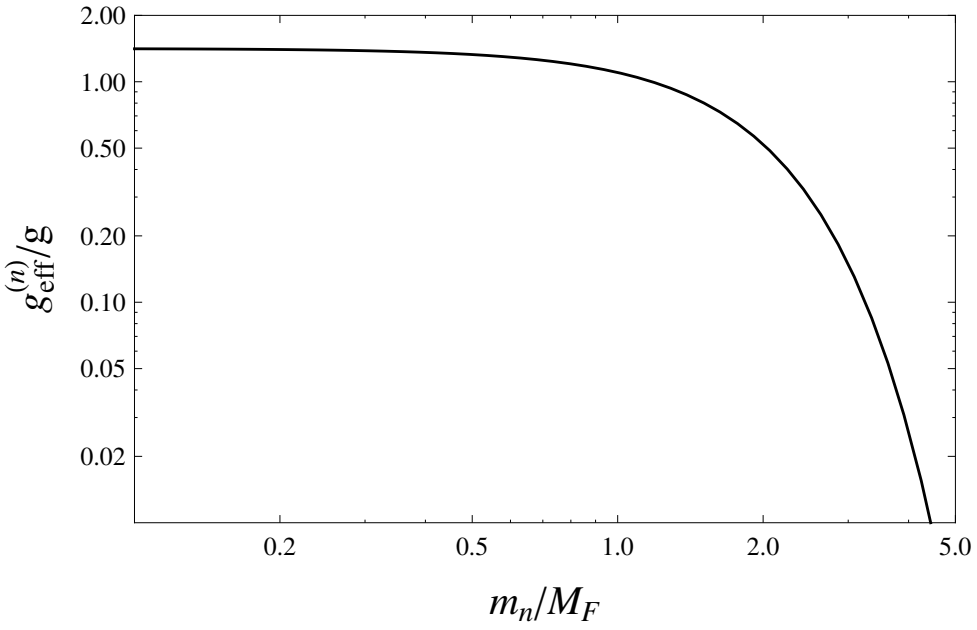

Figure 3.1: The effective coupling ($g_{\rm eff}^{(n)}$) between the n-th KK-mode gauge boson and the chiral fermion as a function of m_n/M_F. The gauge coupling of the zero-mode gauge boson is denoted as g.

universally couple with the fermion. On the other hand, $g_{\rm eff}^{(n)}$ is vanishing in the limit of $M_F \to 0$. This is analogous to the case in the universal extra-dimension model [61], where such couplings are forbidden by the momentum conservation in the 5th coordinate direction.

In Figure 3.1, we show the effective gauge coupling between the n-th KK-mode gauge boson and the chiral fermion. For a narrow width of the domain-wall fermion, the effective gauge coupling approaches to $\sqrt{2}\, g$. As the width of the domain-wall fermion becomes large, the effective coupling is decreasing exponentially. When applied to the SM, the gauge coupling g corresponds to one of the SM gauge couplings and the chiral fermion is identified with an SM fermion. We will discuss implications of this coupling behavior to the LHC phenomenology in the next section.

In 5 dimensions, we may introduce the Yukawa coupling of the SM fermions as

$$\mathcal{L}_Y = -Y_f \overline{D} H S + \text{H.c.} = -Y_f \overline{D_L} H S_R - Y_f \overline{D_R} H S_L + \text{H.c.}, \tag{3.30}$$

where D and S are Dirac fermions in 5 dimensions, whose chiral components, D_L and S_R, are identified as left-handed SM doublet and right-handed singlet fermions under the SM SU(2) gauge group, respectively, by assigning them Z_2-even parities. With the couplings for D and S with the kink background, zero-modes of D_L and S_R are localized around $y = 0$, while zero-modes of D_R and S_L are projected out. The Higgs Lagrangian in Eq. (3.15) is now extended to the SM Higgs doublet case. If we simply set the same couplings for D and S with the kink background, in other words, the common widths of the domain-wall fermions, we obtain an effective Yukawa coupling as the same as Y_f in the 4-dimensional effective theory.

3.3 LHC Phenomenology

The ATLAS and the CMS collaborations have been searching for a new gauge boson resonance with a variety of final states at the LHC Run-2. For the sequential SM Z' and W' bosons, which have the same properties as the SM Z and W bosons except for their masses, the ATLAS collaboration has recently reported their search results with luminosity of about 36 fb^{-1}. The lower bound on the sequential SM Z' boson is obtained to be $m_{Z'} \geq 4.5$ TeV with dilepton final states [63], while $m_{W'} \geq 5.1$ TeV for the sequential SM W' boson mass is obtained with its decay mode $W' \to l\nu$ [64]. In the following, we interpret these results as constraints on the KK-mode gauge bosons in our scenario.

For simplicity, we set a common width $2L$ for the y-dependent SM gauge couplings, so that the KK-mode mass spectra for gluon, weak bosons and photon are approximately the same for $m_{W,Z}^2 \ll m_1^2 = (\pi/L)^2$ (this relation will be justified below). Thus, let us consider the most severe constraint from the W' boson search. Since the total decay width

of W' boson is about 3% of its mass for $m_{W'} \gtrsim 1$ TeV, we employ the narrow-width approximation in evaluating the parton-level cross section of the process,

$$\hat{\sigma}(q\overline{q}' \to W') \propto \Gamma_{W'}(W' \to q\overline{q}')\, \delta(M^2_{\rm inv} - m^2_{W'}) \propto g^2, \tag{3.31}$$

where $M^2_{\rm inv}$ is the invariant mass of the initial partons, $\Gamma_{W'}(W' \to q\overline{q}')$ is the partial decay width into $q\overline{q}'$, and g is the SM SU(2) gauge coupling. When we identify the W' boson with the 1st KK-mode of the SM W boson in the Domain-Wall SM, the only difference is from the effective gauge coupling $g^{(1)}_{\rm eff}$. As shown in Figure 3.1, the effective coupling $g^{(1)}_{\rm eff}$ is a function of the width of the domain-wall fermion. For simplicity, we assume a common width for all SM fermions. Hence, in the narrow-width approximation, we have

$$\sigma(pp \to W^{(1)} \to l\nu) = \left(\frac{g^{(1)}_{\rm eff}}{g}\right)^2 \sigma(pp \to W' \to l\nu), \tag{3.32}$$

by which we can interpret the current ATLAS constraints as those on the 1st KK-mode W boson.

In Figure 3.2, we show the cross section $\sigma(pp \to W^{(1)} \to l\nu)$ as a function of $m_{W'} = m_1$ for various values of $g^{(1)}_{\rm eff}/g$, along with the upper bound on the cross section from the ATLAS results [64] at the LHC RUn-2 with a 36.1 fb^{-1} integrated luminosity (horizontal solid curve (in red)) and the theoretical prediction of $\sigma(pp \to W' \to l\nu)$ for the sequential SM W' boson (dashed line). The solid diagonal lines from left to right depict the theoretical predictions of the cross section $\sigma(pp \to W^{(1)} \to l\nu)$ as a function of m_1 for $g^{(1)}_{\rm eff}/g = 0.04$, 0.1, 0.3 and $\sqrt{2}$, respectively. We see from Figure 3.1 that these $g^{(1)}_{\rm eff}/g$ values correspond to $m_1/M_F = 3.8$, 3.3, 2.5 and 0, respectively. For a fixed $g^{(1)}_{\rm eff}/g$ value, we read off the lower bound on the 1st KK-mode mass from the intersection of the corresponding solid diagonal line and the solid horizontal (red) curve. We find the lower bounds on the 1st KK-mode mass as m_1(TeV) ≥ 1.4, 2.8, 3.9 and 5.5 for $g^{(1)}_{\rm eff}/g = 0.04$, 0.1, 0.3 and $\sqrt{2}$, respectively.

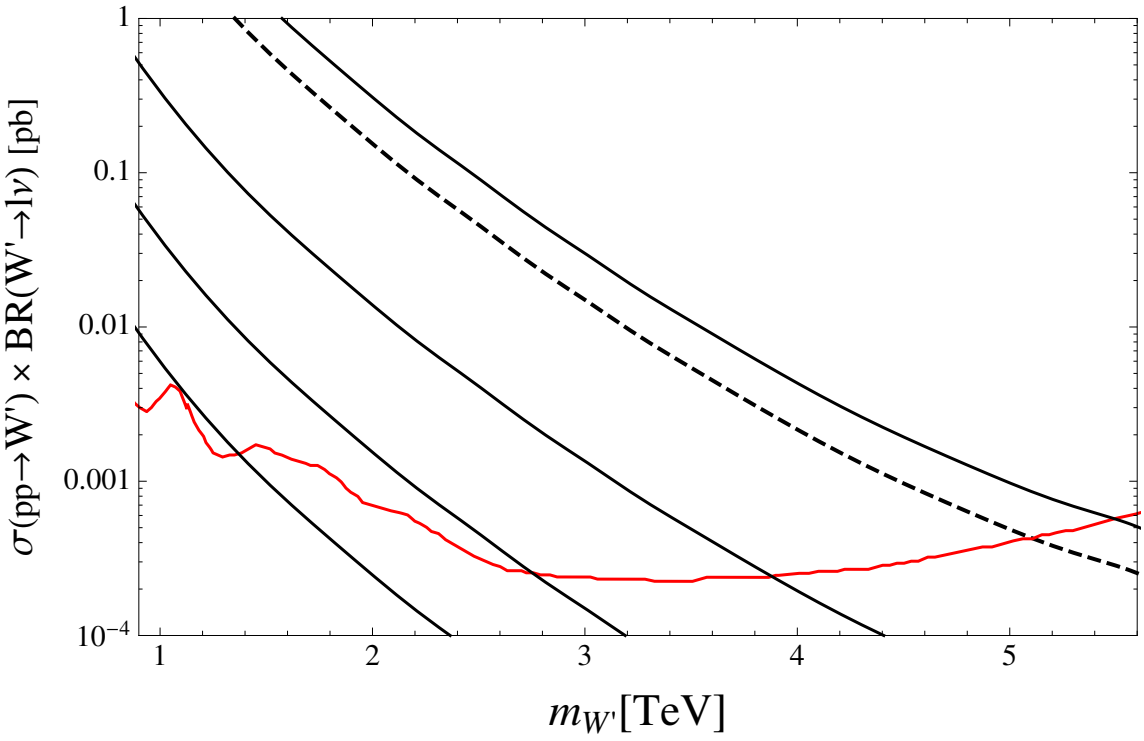

Figure 3.2: The cross section $\sigma(pp \to W^{(1)} \to l\nu)$ as a function of $m_{W'} = m_1$ for $g^{(1)}_{\rm eff}/g =$ 0.04, 0.1, 0.3 and $\sqrt{2}$ (solid diagonal lines) from left to right, along with the theoretical prediction of $\sigma(pp \to W' \to l\nu)$ for the sequential SM W' boson (dashed diagonal line) and the ATLAS results [64] (the cross section upper bound (solid horizontal curve (in red)) at 95% Confidence Level, the expected limit (dotted horizontal curve), $\pm 1\sigma$ expectation (green shaded) and $\pm 2\sigma$ expectation (yellow shaded)).

Let us compare this current LHC bound with constraints imposed by the electroweak precision test (EWPT) measurements. In Ref. [65], the authors have considered the effective four Fermi operators induced by the bulk SM gauge bosons in the Randall-Sundrum (RS) model and have obtained a lower bound on the 1st KK-mode mass as $m_1(\text{TeV}) \geq 23$. In the model the KK-mode coupling is enhanced as $g^{(1)}_{\rm eff}/g \simeq 8.4$. Considering, for example, $g^{(1)}_{\rm eff}/g \simeq \sqrt{2}$ in our model, we can easily interpret the lower bound as $m_1(\text{TeV}) \geq 23 \times \left(\sqrt{2}/8.4\right) \simeq 3.8$. Hence, for this coupling, the current LHC bound is more severe. This is also true for a general choice of $g^{(1)}_{\rm eff}/g$. As another constraint from the EWPT measurements, we consider contributions to the S and T parameters [66] from the KK-modes loop corrections. In our model, the mass spectrum of the gauge and

the Higgs boson KK-modes, as well as their couplings to the SM gauge bosons are the same as those in the Universal Extra Dimension (UED) model [61]. In Ref. [67], the Gfitter Group has studied the S and T parameter constraints for the UED model and obtained a lower bound $m_1(\text{TeV}) \gtrsim 1$ (at 2-σ confidence level). Hence, we can see from Fig. 3.1 that the LHC constraints are more severe than the S and T parameter constraints for $g^{(1)}_{\text{eff}}/g \gtrsim 0.04$.

3.4 Conclusions and discussions

We have proposed a framework to construct "Domain-Wall SM" which is defined in a non-compact 5-dimensional space-time. Considering localization mechanisms for the gauge field, the Higgs field and the chiral fermion in the 5-dimensional Minkowski space, we have derived the 4-dimensional effective Lagrangian for the SM fields and the gauge boson KK-modes. The effective gauge couplings between the KK-modes and the SM chiral fermions are controlled by their domain-wall widths. This geometrical property provides us with an interesting LHC phenomenology on the KK-modes of the SM gauge bosons. We have interpreted the current LHC results from the search for a new gauge boson resonance as the constraints on the Domain-Wall SM.

In the present chapter, we have introduced Z_2-parity under the reflection of the 5th coordinate. This is only for simplifying our formulas and not essential for the construction of the Domain-Wall SM. In the absence of Z_2-parity, we can consider the case that the SM chiral fermions are localized around different points in the 5th dimension. Such a generalization opens up a possibility to solve the fermion mass hierarchy problem in the SM from the wave-function overlapping, leading to an exponentially suppressed effective Yukawa couplings, as proposed in Ref. [31]. In general, such a setup can potentially generate flavor-dependent KK-mode gauge boson couplings and hence the flavor changing neutral currents (FCNCs) mediated by the KK-gauge bosons. It is worth investigating in detail a setup, where fermions are localized in different positions along the extra dimension

direction to naturally reproduce the fermion mass hierarchy while avoiding the FCNC constraints. We leave these considerations for our future work. Configurations of the domain-wall fermions reflect their effective gauge couplings with the KK-mode gauge bosons. Therefore, this "geometry" in the 5th dimension can be tested at the future LHC experiment, once a KK-mode gauge boson is discovered and its coupling to the SM fermions is measured. We may also consider an extension of the Domain-Wall SM, for example, the grand unified theory in non-compact extra-dimensions. There is an interesting proposal in Ref. [68] for a possibility to break the grand unified gauge group into the SM one via domain-wall configurations. Hence, the Domain-Wall SM can provide us with a variety of interesting phenomenologies.

Since graviton resides in the bulk, we also need to consider a localization of graviton to complete our proposal of the Domain-Wall SM. For this purpose, we may combine our scenario with the RS-2 scenario [58] with the Planck brane at $y = 0$. Here we may identify the Planck brane as a domain-wall with the zero-width limit. The mass spectrum of the KK-modes of the SM fields is controlled by the width of the domain-walls, and the current LHC results constrain it to be $\lesssim (1\text{ TeV})^{-1}$. On the other hand, the width of 4-dimensional graviton is controlled by the AdS curvature κ in the RS-2 scenario and its experimental constraint is quite weak, $\kappa \gtrsim 10^{-3}$ eV [58]. Therefore, we can take $\kappa \ll 1$ TeV and neglect the warped background geometry in our setup of the Domain-Wall SM, while the 4-dimensional Einstein gravity is reproduced in the RS-2 scenario at low energies. We may think if the energy density from the SM domain-walls is large and affects the RS-2 background geometry. However, we expect the energy density from the domain-walls of $\mathcal{O}(\Lambda^4)$ with $\Lambda = \mathcal{O}(1\text{ TeV})$, while the energy density of the Planck brane in the RS-2 scenario is given by $\mathcal{O}(M_P^2\kappa^2)$ with the reduced Planck mass of $M_P \simeq 2.4 \times 10^{18}$ GeV. Therefore, we choose the AdS curvature in the range of 10^{-3} eV$\ll \kappa \ll$1 TeV for the theoretical consistency of our scenario.

CHAPTER 4

ASPECTS OF THE DOMAIN WALL STANDARD MODEL

4.1 Introduction

Based on the setup of the Domain-Wall Standard Model in the preceding chapter, in this chapter we investigate various aspects of the Domain-Wall SM in detail. For concreteness, we introduce two solvable examples to localize all the SM fields in certain domains of the 5th dimension, and provide the explicit forms of the KK-mode mass spectrum and eigenfunctions. Among a variety of possible phenomenologies of the Domain-Wall SM, we address the LHC phenomenology of the KK-mode gauge bosons, the Higgs boson phenomenology in the presence of the KK-mode SM fermions, and the KK-mode fermion search at the LHC.

We begin with the localization of the gauge field for two solvable examples and obtain the explicit form for the KK-mode mass spectrum and the KK-mode eigenfunctions. Sec. 4.3 generalizes the localization framework for the Domain-Wall Higgs field and Higgs mechanism. In Sec. 4.4, we consider the Domain-Wall fermions and the 4D effective interactions for the localized SM chiral fermions that were introduced in [32]. This effective theory involves SM fermion interactions with the KK-mode gauge bosons and Higgs bosons. We investigate a variety of phenomenologies for the Domain-Wall SM in Sec. 4.5. The last section is devoted to conclusions and discussions.

4.2 The gauge sector

The Domain-Wall SM has rich phenomenological aspects as we will discuss below. For our phenomenology discussions, we need solvable system that provides us with explicit forms for the gauge boson KK-mode spectrum and eigenfunctions. A simple example is discussed in our previous work [32]. In the following, we introduce two solvable examples, which are much more non-trivial than the example in Ref. [32].

In solving the KK-mode equations in Eq. (3.7), it is convenient to rewrite the equations with a function $f(y)$ defined as $s(y) = f(y)^2$ and introducing new variables,

$$\tilde{\chi}^{(n)}(y) = f(y)\,\chi^{(n)}(y), \quad \tilde{\psi}^{(n)}(x) = f(y)\,\psi^{(n)}(x), \tag{4.1}$$

corresponding to the gauge and the scalar fields. We then have the KK-mode equations which have the form of the Schrödinger equation:

$$\begin{aligned} \left[-\partial_y^2 - G(y)' + G(y)^2\right]\tilde{\chi}^{(n)} &= m_n^2\tilde{\chi}^{(n)}, \\ \left[-\partial_y^2 + G(y)' + G(y)^2\right]\tilde{\psi}^{(n)} &= m_n^2\tilde{\psi}^{(n)}, \end{aligned} \tag{4.2}$$

where $'$ denotes d/dy, and $G(y) = -f(y)'/f(y)$. It is easy to find the zero-mode solution as $\tilde{\chi}^{(0}(y) \propto f(y)$. This result implies that if we have a solvable 1D Quantum Mechanical system resulting in bound states, we adopt this system as our solvable example by identifying $f(y)$ with the ground-state eigenfunction.

4.2.1 Solvable example 1

We now consider the first solvable example which is a Gaussian type function,

$$s(y) = f(y)^2 = M\exp\left[-(m_V y)^2\right], \tag{4.3}$$

where M and m_V are (positive) mass parameters. Substituting it into the KK-mode equations, we obtain

$$\begin{aligned}\left[-\partial_y^2 + m_V^4 y^2\right] \tilde{\chi}^{(n)} &= (m_n^2 + m_V^2)\, \tilde{\chi}^{(n)}, \\ \left[-\partial_y^2 + m_V^4 y^2\right] \tilde{\psi}^{(n)} &= (m_n^2 - m_V^2)\, \tilde{\psi}^{(n)},\end{aligned} \tag{4.4}$$

which are nothing but the Schrödinger equation for the 1D harmonic oscillator,

$$H\Psi^{(n)} = \omega \left(a^\dagger a + \frac{1}{2}\right) \Psi^{(n)} = E_n \Psi^{(n)}, \tag{4.5}$$

with the identifications of the frequency $\omega = 2m_V^2$ and the annihilation/creation operator,

$$a = \frac{1}{\sqrt{2m_V^2}} \left(\frac{d}{dy} + m_V^2 y\right), \quad a^\dagger = \frac{1}{\sqrt{2m_V^2}} \left(-\frac{d}{dy} + m_V^2 y\right). \tag{4.6}$$

Thus, using the energy eigenvalues given by $E_n = 2m_V^2 \left(n + \frac{1}{2}\right)$ $(n = 0, 1, 2, \cdots)$ for the harmonic oscillator, we find the KK-mode spectra for the gauge bosons and the would-be NG modes as $m_n^2 = 2\, n\, m_V^2$ and $m_n^2 = 2(n+1)m_V^2$ for $n = 0, 1, 2, \cdots$, respectively. Note that no zero-mode exists for the scalar field. Shifting $n \to n + 1$ for the scalar mode, we can see the pairing of the massive modes of the gauge bosons and would-be NG modes ($2nm_V^2$ and $\xi\, 2nm_V^2$ for $n = 1, 2, \cdots$). This is nothing but what we expected.

Using the harmonic oscillator algebra, $[a, a^\dagger] = 1$, it is straightforward to obtain the KK-mode functions. For example, the zero-mode function $\tilde{\chi}^{(0)}$ is obtained as a solution of $a\tilde{\chi}^{(0)} = 0$, and the n-th KK-mode function is generated as $\tilde{\chi}^{(n)} \propto (a^\dagger)^n \tilde{\chi}^{(0)}$ by using the zero-mode function. After integrating out the 5th-dimensional degrees of freedom for the Lagrangian of Eq. (3.8), we obtain the 4D effective Lagrangians with the canonically

normalized kinetic terms as

$$\begin{aligned}
\mathcal{L}^4_{\rm gauge} &= \sum_{n=0}^{\infty} \frac{1}{2}\left[\int_{-\infty}^{\infty} s\left(\chi^{(n)}\right)^2\right]\left[A_\mu^{(n)}\left(g^{\mu\nu}(\Box_4 + m_n^2) - \left(1-\frac{1}{\xi}\right)\partial^\mu\partial^\nu\right)A_\nu^{(n)}\right] \\
&= \sum_{n=0}^{\infty} \frac{1}{2}\left[A_\mu^{(n)}\left(g^{\mu\nu}(\Box_4 + m_n^2) - \left(1-\frac{1}{\xi}\right)\partial^\mu\partial^\nu\right)A_\nu^{(n)}\right] \\
\mathcal{L}^4_{\rm scalar} &= -\sum_{n=1}^{\infty} \frac{1}{2}\left[\int_{-\infty}^{\infty} s\left(\psi^{(n)}\right)^2\right]\left[\eta^{(n)}\left(\Box_4 + \xi\, m_n^2\right)\eta^{(n)}\right], \\
&= -\sum_{n=1}^{\infty} \frac{1}{2}\left[\eta^{(n)}\left(\Box_4 + \xi\, m_n^2\right)\eta^{(n)}\right], \qquad (4.7)
\end{aligned}$$

for the KK-mode decomposition,

$$A_\mu(x,y) = \sum_{n=0}^{\infty} A_\mu^{(n)}(x)\chi^{(n)}(y), \quad A_y(x,y) = \sum_{n=1}^{\infty} \eta^{(n)}(x)\chi^{(n-1)}(y). \qquad (4.8)$$

Here, we have changed the label n for the KK-mode decomposition of A_y by $n \to n+1$, and $\psi^{(n)}$ is given by $\psi^{(n)} = \chi^{(n-1)}$ for $n = 1, 2, \cdots$. The explicit form of the first three KK-mode functions are

$$\begin{aligned}
\chi^{(0)}(y) &= g, \\
\chi^{(1)}(y) &= \sqrt{2}\, g\,(m_V y), \\
\chi^{(2)}(y) &= \frac{g}{\sqrt{2}}\left(1 - 2(m_V y)^2\right), \\
\chi^{(3)}(y) &= \frac{g}{\sqrt{3}}(m_V y)\left(3 - 2(m_V y)^2\right), \qquad (4.9)
\end{aligned}$$

where g is the U(1) gauge coupling in the 4D effective theory defined by $g = \pi^{-1/4}\sqrt{m_V/M}$.

4.2.2 Solvable example 2

As the second example, we consider

$$s(y) = f(y)^2 = \frac{M}{[\cosh(m_V y)]^{2\gamma}}, \qquad (4.10)$$

where M and m_V are positive mass parameters, and γ is a positive constant. We then express Eq. (4.2) as

$$\left[-\partial_y^2 - \frac{\gamma(\gamma+1)m_V^2}{\cosh^2(m_V y)}\right]\tilde{\chi}^{(n)} = \left(m_n^2 - \gamma^2 m_V^2\right)\tilde{\chi}^{(n)},$$
$$\left[-\partial_y^2 - \frac{\gamma(\gamma-1)m_V^2}{\cosh^2(m_V y)}\right]\tilde{\psi}^{(n)} = \left(m_n^2 - \gamma^2 m_V^2\right)\tilde{\psi}^{(n)}. \tag{4.11}$$

These equations have the form of the Schrödinger equation, $(-\partial_y^2 + V)\Psi^{(n)} = E_n\Psi^{(n)}$. Since the potential corresponds to $V \propto -1/\cosh^2(m_V y) < 0$, we expect the existence of a bound state with $E_n < 0$.

We are interested in the localization of the gauge field, namely, bound states from the the Schrödinger equation satisfying the following boundary conditions: $|\tilde{\chi}^{(n)}(0)| < \infty$ for $y \to 0$, and $\tilde{\chi}^{(n)}(y) \to 0$ for $|y| \to \infty$. Such solutions are described by using the hyper-geometric function $F[a, b; c; y]$ [62]. We find the eigenvalues for $\tilde{\chi}^{(n)}$ as

$$m_n^2 = n\,(2\gamma - n)\,m_V^2 \quad (n = 0, 1, 2, \cdots < \gamma). \tag{4.12}$$

The number of (localized) KK-modes is terminated by a condition $E_n = m_n^2 - \gamma^2 m_V^2 < 0$, and thus a massive mode exists for $\gamma > 1$. The eigenfunctions for even numbers of $n = 2n'$ ($n' = 0, 1, 2, \ldots$) and odd numbers of $n = 2n'' + 1$ ($n'' = 0, 1, 2, \ldots$) are given by (up to normalization factor)

$$\tilde{\chi}^{(n')}(y) = [\cosh(m_V y)]^{-\gamma}\; F\left[-n', -\gamma + n'; 1/2; 1 - \cosh^2(m_V y)\right], \tag{4.13}$$

and

$$\tilde{\chi}^{(n'')}(y) = \sinh(m_V y)\,[\cosh(m_V y)]^{-\gamma}\, F\left[-n'', -\gamma + n'' + 1; 3/2; 1 - \cosh^2(m_V y)\right], \tag{4.14}$$

respectively.

Similarly, for the scalar field we impose the boundary conditions: $|\tilde{\psi}^{(n)}(0)| < \infty$ for $y \to 0$, and $\tilde{\psi}^{(n)}(y) \to 0$ for $|y| \to \infty$. We can easily find the eigenfunctions of $\tilde{\psi}^{(n)}$ as follows. Substituting $\gamma = \overline{\gamma} + 1$ and $m_n^2 = \overline{m_n}^2 + (2\overline{\gamma} + 1)m_V^2$ into the second equations, we obtain

$$\left[-\partial_y^2 - \frac{\overline{\gamma}(\overline{\gamma}+1)m_V^2}{\cosh^2(m_V y)}\right] \tilde{\psi}^{(n)} = \left(\overline{m_n}^2 - \overline{\gamma}^2 m_V^2\right) \tilde{\psi}^{(n)}, \tag{4.15}$$

which is identical to the equation for $\tilde{\chi}^{(n)}$. Thus, the eigenvalues for $\tilde{\psi}^{(n)}$ are given by

$$m_n^2 = (n+1)\left(2\gamma - (n+1)\right) m_V^2 \quad (n = 0, 1, 2, \cdots < \gamma - 1). \tag{4.16}$$

As for the first example, no zero-mode exists for the scalar mode, and we can see the pairing of the KK-mode mass spectrum between the gauge fields and the corresponding would-be NG modes. The eigenfunctions for even numbers of $n = 2n'$ ($n' = 0, 1, 2, \ldots$) and odd numbers of $n = 2n'' + 1$ ($n'' = 0, 1, 2, \ldots$) are given by (up to normalization factor)

$$\tilde{\psi}^{(n')}(y) = [\cosh(m_V y)]^{-\gamma+1}\ F\left[-n', -\gamma + n' + 1; 1/2; 1 - \cosh^2(m_V y)\right], \tag{4.17}$$

and

$$\tilde{\psi}^{(n'')}(y) = \sinh(m_V y)\,[\cosh(m_V y)]^{-\gamma+1}\, F\left[-n'', -\gamma + n'' + 2; 3/2; 1 - \cosh^2(m_V y)\right], \tag{4.18}$$

respectively.

Unlike the first example, we have a finite number of the localized KK-modes in the second example. For concreteness, let us fix $\gamma = 2$. In this case, we have only one KK-mode gauge boson with the mass eigenvalue $m_1^2 = 3m_V^2$. In the 4D effective theory with the canonically normalized kinetic terms like Eq. (4.7), the explicit form of the

KK-mode expansions is given by

$$\begin{aligned} A_\mu(x,y) &= g\, A_\mu^{(0)}(x) + \sqrt{2}\, g\, \sinh(m_V y)\, A_\mu^{(1)}(x), \\ A_y(x,y) &= \sqrt{\frac{2}{3}}\, g\, \cosh(m_V y)\, \eta^{(1)}(x), \end{aligned} \tag{4.19}$$

where the gauge coupling in the 4D effective theory is defined as $g = \sqrt{\frac{3m}{4M}}$.

It is straightforward to extend the U(1) gauge theory to the SM case. For the SM gauge group of $\mathrm{SU}(3)_c \times \mathrm{SU}(2)_L \times \mathrm{U}(1)_Y$, we introduce three y-dependent gauge couplings in the original 5D Lagrangian. Let us call them as $s_i(y)$ for $i = 1, 2, 3$ corresponding to the three gauge groups. For simplicity, we set $s_1 \propto s_2$ in this chapter, so that the KK-mode spectrum for the $\mathrm{SU}(2)_L \times \mathrm{U}(1)_Y$ gauge bosons are the same. As we will see in the next section, this choice simplifies our calculation of the KK-mode mass spectrum after the electroweak symmetry breaking.

4.3 The Higgs sector

Next we reconsider the 5D Higgs sector of the Abelian Higgs model originally discussed in Ref. [32], where the following consideration utilizes a general $s_H(y)$ initially. The Lagrangian for the Higgs sector of the form,

$$\mathcal{L}_5^H = s_H(y) \left[(\mathcal{D}^M H)^\dagger (\mathcal{D}_M H) - \frac{1}{2}\lambda_H \left(H^\dagger H - \frac{v^2}{2} \right)^2 \right], \tag{4.20}$$

where H is the Higgs field, v is its VEV, λ_H is a Higgs quartic coupling, and the covariant derivative is given by $\mathcal{D}_M = \partial_M - iQ_H A_M$ with a U(1) charge Q_H for the Higgs field. Here, we have introduced a $y-$dependent kinetic term $s_H(y)$. In our convention, the Higgs field and s_H have mass dimension one.

Expanding about the vacuum $H = (v + h + i\phi)/\sqrt{2}$ and neglecting the interaction

terms, we obtain (up to total derivative terms)

$$\begin{aligned}\mathcal{L}_5^H &\supset \frac{1}{2}s_H\left[(\partial^M h)(\partial_M h) - m_h^2 h^2\right] + \frac{1}{2}s_H(\partial^M\phi)(\partial_M\phi) \\ &= -\frac{1}{2}s_H h(\Box_4 + m_h^2)h + \frac{1}{2}h\,\partial_y(s_H\partial_y h) - \frac{1}{2}s_H\phi\Box_4\phi + \frac{1}{2}\phi\,\partial_y(s_H\partial_y\phi), \quad (4.21)\end{aligned}$$

where $m_h^2 = \lambda_H v^2$ is the physical Higgs boson mass. Applying the KK-mode decomposition to these fields,

$$h(x,y) = \sum_{n=0}^{\infty} h^{(n)}(x)\,\chi_h^{(n)}(y), \quad \phi(x,y) = \sum_{n=0}^{\infty}\phi^{(n)}(x)\,\chi_\phi^{(n)}(y), \quad (4.22)$$

we see that the KK-mode equations for $\chi_h^{(n)}$ and $\chi_\phi^{(n)}$ are identical to that of the gauge boson in Eq. (3.7) with the replacement by $s(y) \to s_H(y)$. Since the zero-mode $\phi^{(0)}$ is the would-be NG mode eaten by $A_\mu^{(0)}$, the theoretical consistency requires the configurations of $\phi^{(0)}$ and $A_\mu^{(0)}$ to be identical. With the solutions of the KK-mode equations, the free Lagrangian for the scalar fields in the 4D effective theory is described as

$$\mathcal{L}_4^H \supset -\frac{1}{2}\sum_{n=0}^{\infty}\left[\int_{-\infty}^{\infty} dy\, s_H\left(\chi_h^{(n)}\right)^2\right]\left[h^{(n)}\left(\Box_4 + (m_h^2 + m_n^2)\right)h^{(n)} + \phi^{(n)}(\Box_4 + m_n^2)\phi^{(n)}\right], \quad (4.23)$$

where we have used $\chi_h^{(n)}(y) = \chi_\phi^{(n)}(y)$ since their equations are identical. After canonically normalizing kinetic terms, the KK-mode decomposition with respect to physical Higgs bosons is formally given by $h(x,y) = h^{(0)}(x) + \chi_h^{(n)}(y)\,h^{(n)}(x)$, where we have scaled the KK-mode functions so as to satisfy

$$\int_{-\infty}^{\infty} dy\, s_H\left(\chi_h^{(n)}\right)^2 = 1 \quad (n = 0, 1, 2...). \quad (4.24)$$

Recall that $\chi_h^{(0)}$ is a constant. The U(1) gauge symmetry is broken by $\langle H\rangle = v/\sqrt{2}$, from which the masses for the U(1) gauge bosons in the 4D effective theory are generated. Their

mass terms are given by

$$\mathcal{L}_4^H \supset \frac{1}{2}Q_H^2 v^2 \sum_{n,m=0}^{\infty} \left[\int_{-\infty}^{\infty} dy\, s_H(y) \chi^{(n)}(y) \chi^{(m)}(y) \right] \eta^{\mu\nu} A_\mu^{(n)}(x) A_\nu^{(m)}(x). \tag{4.25}$$

This formula indicates that the KK-mode gauge bosons, $A_\mu^{(n)}$ and $A_\mu^{(m)}$ $(n \neq m)$, have a mixing mass in general, and the analysis of the gauge boson mass spectrum is complicated. For simplicity, let us take $s_H(y) \propto s(y)$ in this chapter, so that no mixing mass is generated because of the orthogonal condition,

$$\int_{-\infty}^{\infty} dy\, s_H(y) \chi^{(n)}(y) \chi^{(m)}(y) \propto \int_{-\infty}^{\infty} dy\, s(y) \chi^{(n)}(y) \chi^{(m)}(y) = 0, \tag{4.26}$$

for $n \neq m$. After normalizing the kinetic terms for the zero-mode and KK-mode gauge bosons, we find the mass spectrum as

$$m_A^{(0)} = Q_H\, g\, v, \quad m_A^{(n)} = \sqrt{m_n^2 + \left(m_A^{(0)}\right)^2}, \tag{4.27}$$

for the zero-mode and the KK-modes $(n = 1, 2, \cdots)$, respectively. Here we have obtained the zero-mode gauge boson mass of the same form as the one in the Abelian Higgs model in 4D.

We now extend the model to the SM case. As we mentioned in the previous section, we set $s_1 \propto s_2$, so that the KK-mode spectrum of the $\mathrm{SU}(2)_L \times \mathrm{U}(1)_Y$ gauge bosons are the same. The Higgs field in the Abelian Higgs model is extended to the SM Higgs doublet field. After the electroweak symmetry breaking we have the gauge boson (photon (γ), W boson and Z boson) mass spectrum: for the zero-modes,

$$m_\gamma = 0, \;\; m_W = \frac{1}{2} g_2 v, \;\; m_Z = \frac{1}{2} g_Z v, \tag{4.28}$$

where $g_Z = \sqrt{g_2^2 + g_Y^2}$ with g_2 and g_Y being the $\mathrm{SU}(2)_L$ and $\mathrm{U}(1)_Y$ gauge couplings,

respectively, and $v_h = 246$ GeV is the Higgs doublet VEV, while their KK-mode mass spectrum is given by

$$m_\gamma^{(n)} = m_n, \;\; m_W^{(n)} = \sqrt{m_n^2 + m_W^2}, \;\; m_Z^{(n)} = \sqrt{m_n^2 + m_Z^2}. \tag{4.29}$$

4.4 Domain-wall fermions

In this section, we consider localized chiral fermions, whose zero-modes are identified with the SM chiral fermions. Again, we consider the U(1) gauge theory to simplify our discussion, which can be easily extended to the 5D SM case. We follow a mechanism in Ref. [38] to generate the domain-wall fermion in 5D space-time and first introduce a real scalar field ($\varphi(x, y)$) in the 5D bulk:

$$\mathcal{L}_{(5)} = \frac{1}{2} \left(\partial_M \varphi\right) \left(\partial^M \varphi\right) - V(\varphi) \; , \tag{4.30}$$

where the scalar potential is give by

$$V(\varphi) = \frac{m_\varphi^4}{2\lambda} - m_\varphi^2 \varphi^2 + \frac{\lambda}{2} \varphi^4. \tag{4.31}$$

It is well known that there is a non-trivial background configuration $\varphi_0(y)$ as a solution of the equation of motion, namely, the so-called kink solution,

$$\varphi_{\rm kink}(y) = \frac{m_\varphi}{\sqrt{\lambda}} \tanh[m_\varphi y]. \tag{4.32}$$

Here, we have chosen the kink center at $y = 0$, for simplicity. Expanding the scalar around the kink background, $\varphi(x, y) = \varphi_{\rm kink}(y) + U_\varphi(y)\tilde{\varphi}(x)$, we can solve the linearized equation of motion. It is easy to notice that this system is the same as the second solvable example

in Sec. 4.2 with $\gamma = 2$, so that we have the solution [70]:

$$\varphi(x,y) = \varphi_{\rm kink}(y) + \frac{\sqrt{3m_\varphi}}{2}\left[\frac{1}{\cosh^2(m_\varphi y)}\right]\varphi^{(0)}(x) + \sqrt{\frac{3m_\varphi}{2}}\left[\frac{\sinh(m_\varphi y)}{\cosh^2(m_\varphi y)}\right]\varphi^{(1)}(x), \quad (4.33)$$

where $\varphi^{(0)}(x)$ is a massless NG mode corresponding to the spontaneous breaking of the translational invariance in the 5th dimension, and $\varphi^{(1)}(x)$ is a massive mode with a mass $m_\varphi^{(1)} = \sqrt{3}m_\varphi$. Here, the kinetic terms for the eigenstates are canonically normalized.

Following our discussion of the DW fermions from [32], the general solution to Eq. (3.24) can be found even without introducing a Z_2 symmetry for this setup. For our phenomenology discussion in the next section, let us set $Y/\sqrt{\lambda} = 2$. In this case, we have only one KK-mode Dirac fermion in the 4D effective theory with mass $\sqrt{3}m_\varphi$. The KK-mode expansion is explicitly described as

$$\begin{aligned}
\psi_L(x,y) &= \frac{\sqrt{3m_\varphi}}{2}\left[\frac{1}{\cosh^2(m_\varphi(y-y_0))}\right]\psi_L^{(0)}(x) + \sqrt{\frac{3m_\varphi}{2}}\left[\frac{\sinh(m_\varphi(y-y_0))}{\cosh^2(m_\varphi(y-y_0))}\right]\psi_L^{(1)}(x), \\
\psi_R(x,y) &= \sqrt{\frac{m_\varphi}{2}}\left[\frac{1}{\cosh(m_\varphi(y-y_0))}\right]\psi_R^{(1)}(x), \qquad (4.34)
\end{aligned}$$

for which the kinetic terms are canonically normalized. Here, we have generalized the system and set the kink center at y_0.

Let us now describe the Lagrangian for the chiral fermion in the 4D effective theory as

$$\mathcal{L}_4 \supset \overline{\psi_L^{(0)}} i\gamma^\mu \left(\partial_\mu - iQ_f g A_\mu^{(0)}\right)\psi_L^{(0)} + \sum_{n=1}^{\infty} Q_f\, g_{\rm eff}^{(n)}\, A_\mu^{(n)}\left[\overline{\psi_L^{(0)}}\gamma^\mu\psi_L^{(0)}\right], \quad (4.35)$$

where the 4D effective gauge coupling between the chiral fermion and the n-th KK-mode gauge boson is given by

$$g_{\rm eff}^{(n)} = \int_{-\infty}^{\infty} dy \left(\chi_L^{(0)}\right)^2 \chi^{(n)}. \quad (4.36)$$

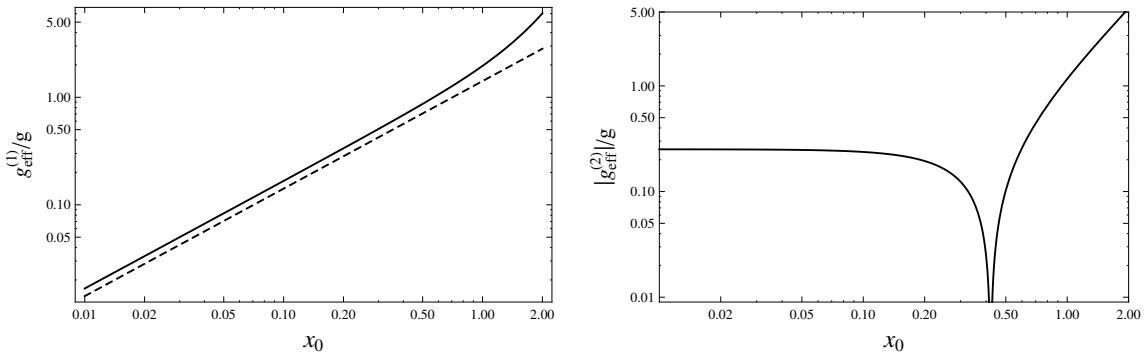

Figure 4.1: Left: The effective coupling ($g^{(1)}_{\rm eff}$) between the 1st KK-mode gauge boson and the chiral fermion as a function of x_0 for the first (solid) and second (dashed) examples in Sec. 4.2. The gauge coupling of the zero-mode gauge boson is denoted as g. Right: The effective coupling ($g^{(2)}_{\rm eff}$) of the 2nd KK-mode gauge boson with the chiral fermion as a function of x_0 for the second example in Sec. 4.2. For $x_0 > 0.421$, we find $g^{(2)}_{\rm eff} < 0$.

For simplicity, we consider the solvable examples in Sec. 4.2 and take $m_V = m_\varphi$. For the first and second examples, the effective gauge couplings of the 1st KK-mode gauge boson are, respectively, given by

$$\begin{aligned}
\text{Example 1}: \ \frac{g^{(1)}_{\rm eff}}{g} &= \frac{3\sqrt{2}}{4}\, m_\varphi^2 \int_{-\infty}^{\infty} dy\, \frac{y}{\cosh^4(m_\varphi(y-y_0))} \\
&= \frac{3\sqrt{2}}{4} \int_{-\infty}^{\infty} dx\, \frac{x}{\cosh^4(x-x_0)}, \\
\text{Example 2}: \ \frac{g^{(1)}_{\rm eff}}{g} &= \frac{3\sqrt{2}}{4}\, m_\varphi \int_{-\infty}^{\infty} dy\, \frac{\sinh(m_\varphi y)}{\cosh^4(m_\varphi(y-y_0))} \\
&= \frac{3\sqrt{2}}{4} \int_{-\infty}^{\infty} dx\, \frac{\sinh(x)}{\cosh^4(x-x_0)},
\end{aligned} \tag{4.37}$$

where $x_0 = m_\varphi y_0$. Since the eigenfunction of the 1st KK-mode gauge boson is an odd-function of y, the effective coupling vanishes $g^{(1)}_{\rm eff}/g \to 0$ for $x_0 \to 0$. In the first example, there is an infinite tower of KK-modes, and we also calculate the effective gauge coupling of the 2nd KK-mode gauge boson,

$$\frac{g^{(2)}_{\rm eff}}{g} = \frac{3}{4\sqrt{2}}\, m_\varphi \int_{-\infty}^{\infty} dy\, \frac{1-2(m_\varphi y)^2}{\cosh^4(m_\varphi(y-y_0))} = \frac{3}{4\sqrt{2}} \int_{-\infty}^{\infty} dx\, \frac{1-2x^2}{\cosh^4(x-x_0)}, \tag{4.38}$$

which approaches $g^{(2)}_{\rm eff}/g \to 0.251$ for $x_0 \to 0$.

In Figure 4.1, we show the effective gauge couplings between the 1st KK-mode gauge boson and the chiral fermion for the first (solid) and second (dashed) examples (left panel), and the effective gauge coupling of the 2nd KK-mode gauge boson with the chiral fermion (right panel). In the left panel, the gauge couplings vanish for $x_0 \to 0$, while the gauge coupling of the 2nd KK-mode approaches a constant value, $g^{(2)}_{\rm eff}/g \to 0.251$. We find $g^{(2)}_{\rm eff} < 0$ for $x_0 > 0.421$. When applied to the SM, the gauge coupling g corresponds to one of the SM gauge couplings and the chiral fermion is identified with an SM fermion. We will discuss implications of this coupling behavior to LHC phenomenology in the next section.

Finally, let us extend our system to the SM case, and we introduce the Yukawa coupling of the SM fermions in 5D as

$$\mathcal{L}_Y = -Y_f \overline{D} H S + \text{H.c.} = -Y_f \overline{D_L} H S_R - Y_f \overline{D_R} H S_L + \text{H.c.}, \tag{4.39}$$

where D and S are 5D fermions of the SM SU(2) doublet and singlet, respectively, we have decomposed them into their chiral components $D = D_L + D_R$ and $S = S_L + S_R$, and H is the 5D Higgs doublet. With the kink background, zero-modes of D_L and S_R are identified with left-handed SM doublet and right-handed singlet fermions. For simplicity, suppose the KK-mode expansions for D and S (we exchange the chiraliteis for S) are given by Eq. (4.34). For the Higgs doublet field in 5D, let us take, for simplicity,

$$s_H(y) = \frac{3}{4} \frac{m_\varphi}{\cosh^4(m_\varphi y)} \tag{4.40}$$

as in Sec. 4.2, so that the KK-mode decomposition of the physical Higgs boson after the electroweak symmetry breaking are given by (see Eq. (4.19))

$$h(x,y) = h^{(0)}(x) + \sqrt{2} \sinh(m_\varphi y)\, h^{(1)}(x). \tag{4.41}$$

When we identify Eq. (4.39) with top Yukawa coupling in 5D, we obtain a 4D effective Yukawa coupling for the top quark as

$$\mathcal{L}_Y^4 \supset -m_t \left(1 + \frac{h^{(0)}}{v}\right) \overline{t_L} t_R - \left(\frac{m_t}{v}\right) C_{\text{eff}}\, h^{(1)}\, \overline{t_L} t_R, \tag{4.42}$$

where $m_t = Y_f v/\sqrt{2}$, and C_{eff} is given by Eq. (4.37). The top quark mass formula is the same as the SM in 4D, while the model involves a KK-mode Higgs boson with the Yukawa coupling, $m_t C_{\text{eff}}/v$ and its mass $\sqrt{3m_\varphi^2 + m_h^2}$ with $m_h = 125$ GeV.

4.5 KK-mode Phenomenology

Prediction of the KK-modes in the 4D effective theory is a common property of extra-dimensional models and we can investigate the phenomenology involving the KK-modes. However, in the Domain-Wall SM, the KK-mode spectra and the coupling manner of each KK-mode with the SM particles depend on the localization mechanism. This property is in sharp contrast to, for example, the Universal Extra-Dimension model [61], where the KK-mode eigenfunctions are uniquely determined by boundary conditions associated with the compactification of the 5th dimension. The Domain-Wall SM offers more variety of the KK-mode phenomenologies than usual compactified extra-dimensional models, thanks to rich geometrical structures of the localized SM particles and their KK-modes. In this section, we address a few directions for interesting KK-mode phenomenologies.

4.5.1 Phenomenology of KK-mode gauge bosons

The ATLAS and the CMS collaborations have been searching for a new gauge boson resonance with a variety of final states at the LHC Run-2. The so-called sequential SM Z' and W' bosons, which have the same properties as the SM Z and W bosons except for their masses, have been examined as a benchmark model. According to a recent report by the ATLAS collaboration on their search results with luminosities of about 36 fb^{-1}, the

lower mass bound on the sequential SM Z' boson is $m_{Z'} \geq 4.5$ TeV, which is obtained by the search with dilepton final states [63]. A little more severe constraint, $m_{W'} \geq 5.1$ TeV, is obtained for the sequential SM W' boson mass from the search with its decay mode $W' \to l\nu$ [64]. In this subsection, we interpret these results as constraints on the KK-mode gauge bosons in the Domain-Wall SM.

In Sec. 4.2, we have chosen $s_1 \propto s_2$, so that the mass spectrum of the KK-mode Z and W bosons are the same, neglecting the mass terms generated by the electroweak symmetry breaking. Thus, we consider the most severe constraint from the W' boson search. Since the total decay width of the sequential W' boson is about 3% of its mass for $m_{W'} \gtrsim 1$ TeV, we employ the narrow-width approximation in evaluating the parton-level cross section of the process,

$$\hat{\sigma}(q\overline{q'} \to W') \propto \Gamma_{W'}(W' \to q\overline{q'})\, \delta(M^2_{\rm inv} - m^2_{W'}) \propto g^2, \tag{4.43}$$

where $M^2_{\rm inv}$ is the invariant mass of the initial partons, $\Gamma_{W'}(W' \to q\overline{q'})$ is the partial decay width into $q\overline{q'}$, and g is the SM SU(2) gauge coupling. The difference of the sequential W' boson and the KK-mode W boson in the Domain-Wall SM is only the coupling constant. Because of the non-trivial eigenfunctions of the SM fermions and the KK-mode W boson, the effective gauge coupling constant is not the same as the SM gauge coupling constant, as shown in Figure 4.1 for our example. Hence, we have a relation between the production cross sections of the sequential W' and the 1st KK-mode W bosons in the narrow-width approximation:

$$\sigma(pp \to W^{(1)} \to l\nu) = \left(\frac{g^{(1)}_{\rm eff}}{g}\right)^2 \sigma(pp \to W' \to l\nu), \tag{4.44}$$

by which we can interpret the current ATLAS constraints as those on the 1st KK-mode W boson ($W^{(1)}$).

In Figure 4.2, we show the cross section $\sigma(pp \to W^{(1)} \to l\nu)$ as a function of

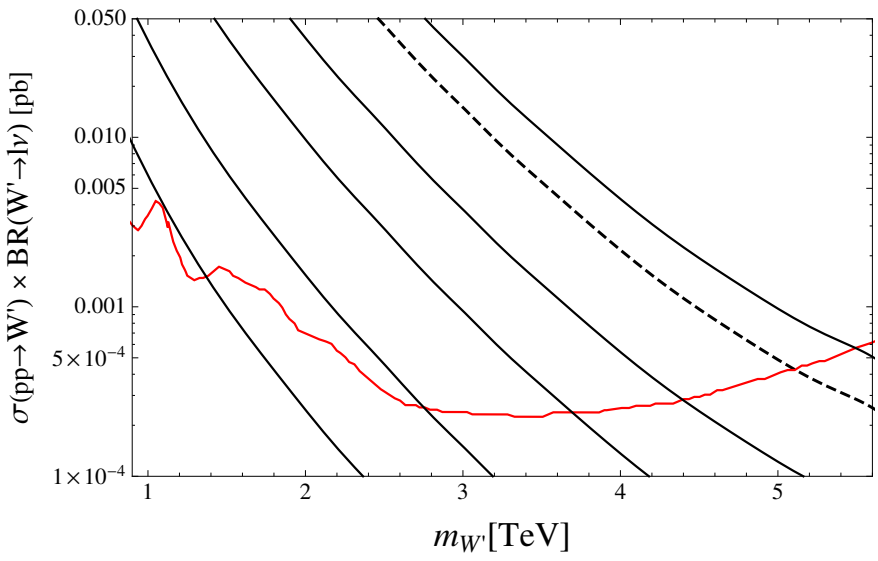

Figure 4.2: The cross section $\sigma(pp \to W^{(1)} \to l\nu)$ as a function of $m_{W'} = m^{(1)}_{W'}$ for $g^{(1)}_{\rm eff}/g =$ 0.04, 0.1, 0.251, 0.5 and $\sqrt{2}$ (solid lines) from left to right, along with the upper bound on the cross section from the ATLAS results (horizontal curve (in red)) and the theoretical prediction of $\sigma(pp \to W' \to l\nu)$ for the sequential SM W' boson (dashed line). For these $g^{(1)}_{\rm eff}/g$ values, we find the lower bounds on the 1st KK-mode W boson as $m^{(1)}_{W'}$[TeV] $\geq$ 1.4, 2.8, 3.7 4.4 and 5.5, respectively. The result for $g^{(1)}_{\rm eff}/g = 0.251$ can be identified as the result for the 2nd KK-mode W boson in the limit of $x_0 \to 0$.

$m_{W'} = m^{(1)}_{W'}$ for various values of $g^{(1)}_{\rm eff}/g$, along with the upper bound on the cross section from the ATLAS results [64] (horizontal curve (in red)) and the theoretical prediction of $\sigma(pp \to W' \to l\nu)$ for the sequential SM W' boson (dashed line). The solid diagonal lines from left to right depict the theoretical predictions of the cross section $\sigma(pp \to W^{(1)} \to l\nu)$ for $g^{(1)}_{\rm eff}/g = 0.04$, 0.1, 0.251, 0.5 and $\sqrt{2}$, respectively, corresponding to $x_0 = 0.024$, 0.060, 0.15, 0.30 and 0.77 ($x_0 = 0.028$, 0.071, 0.18, 0.35 and 1.0) from the solid (dashed) line in the left panel of Figure 4.1. For these $g^{(1)}_{\rm eff}/g$ values, we read off the lower bounds on the 1st KK-mode mass as $m^{(1)}_{W'}$[TeV] $\geq$ 1.4, 2.8, 3.7 4.4 and 5.5, respectively. The result for $g^{(1)}_{\rm eff}/g = 0.251$ is identified with the result for the 2nd KK-mode gauge boson for $x_0 \to 0$ from the right panel of Figure 4.1.

The structure of the KK-modes depend on a localization mechanism, in particular, the shape of y-dependent gauge couplings. We have introduced two solvable examples in

Sec. 4.2: the first one predicts an infinite tower of KK-modes, while the KK-mode expansion is terminated in the second example. The second example is in sharp contrast to extra-dimensional models with compactified extra-dimensions, which predict the infinite tower of KK-mode spectrum. Once the 1st KK-mode state is discovered, the search for higher KK-mode states at high energy colliders can test if an extra-dimension is compactified or not.

4.5.2 Higgs boson phenomenology

Since the KK-modes of the SM particles have couplings with the SM Higgs boson, the presence of the KK-modes affects on Higgs boson phenomenology. In particular, the Higgs boson properties measured at the LHC [71] are altered from the SM predictions. In this section, we consider implication of the KK-modes of top quark and W boson to the Higgs boson phenomenology. See, for example, Ref. [72], for a pioneering work of this direction.

The SM Higgs boson has effective couplings with digluon and diphoton of the form,

$$\mathcal{L}_{\rm Higgs-gauge} = C_{gg}\, h\, G^A_{\mu\nu} G^{A\mu\nu} + C_{\gamma\gamma}\, h\, F_{\mu\nu} F^{\mu\nu}, \tag{4.45}$$

where $G^A_{\mu\nu}$ $A = 1, 2, \cdots, 8$ and $F_{\mu\nu}$ are the field strengths of gluon and photon. In the SM, these effective operators are induced dominantly through 1-loop corrections of top quark and W-boson (and associated would-be NG bosons and ghosts) [73]. The effective coupling with digluon from top quark loop corrections is calculated to be

$$C^{\rm SM}_{gg} = \frac{\alpha_{\rm s}}{16\pi v} F_{1/2}(\tau_t), \tag{4.46}$$

where α_s is the QCD coupling, and $\tau_t = 4m_t^2/m_h^2$ with top quark mass m_t, and Higgs boson mass m_h. The effective coupling with diphoton is from1-loop corrections with top quark

and W-boson, and we have

$$C_{\gamma\gamma}^{\rm SM} = \frac{\alpha_{\rm em}}{8\pi v}\left(\frac{4}{3}F_{1/2}(\tau_t) + F_1(\tau_W)\right), \tag{4.47}$$

where $\tau_W = 4m_W^2/m_h^2$ with the W-boson mass m_W. The explicit formulas of the loop functions are given by

$$F_{1/2}(\tau) = 2\tau\left[1 + (1-\tau)\, f(\tau)\right], \quad F_1(\tau) = -\left[2 + 3\tau + 3\tau\,(2-\tau)\, f(\tau)\right], \tag{4.48}$$

with $f(\tau) = \left[\sin^{-1}\left(1/\sqrt{\tau}\right)\right]^2$ $(\tau > 1)$. For $m_t = 173.34$ GeV [74], $m_W = 80.4$, and $m_h = 125.09$ GeV [71], we find $F_{1/2}(\tau_t) \simeq 1.38$ and $F_1(\tau_W) \simeq -8.33$.

In the presence of the KK-mode top quarks and W bosons, the effective Higgs couplings receive 1-loop corrections with the KK-modes. Again, we consider the KK-mode expansions in Eq. (4.34) for top quarks of the SM SU(2) doublet component and the SU(2) singlet. After the electroweak symmetry breaking, it is easy to derive the mass matrix for the 1st KK-mode top quarks as

$$\mathcal{M}_t = \begin{bmatrix} -m_t^{(1)} & m_t \\ m_t & m_t^{(1)} \end{bmatrix}, \tag{4.49}$$

where $m_t^{(1)} = \sqrt{3}m_\varphi$ is the KK-mode mass. We then have degenerate mass eigenvalues, $m_{\rm KK} = \sqrt{\left(m_t^{(1)}\right)^2 + m_t^2}$. For $m_{\rm KK}^2 \gg m_h^2$, we can easily calculate the contribution of the KK-mode top quarks to C_{gg} by using the Higgs low-energy theorem [73] as

$$C_{gg}^{\rm KK-top} \simeq \frac{\alpha_{\rm s}}{8\pi v} b_3^t \frac{\partial}{\partial \log v}\log(m_{\rm KK}) \times 2 \simeq \frac{\alpha_{\rm s}}{6\pi v}\left(\frac{m_t}{m_{\rm KK}}\right)^2, \tag{4.50}$$

where $b_3^t = 2/3$ is the top quark contribution to the beta function coefficient of QCD.

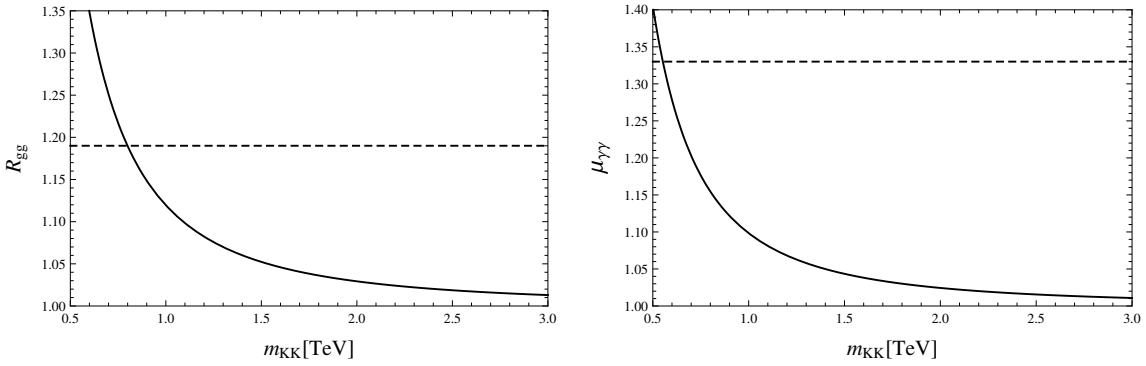

Figure 4.3: Left: The ratio of the Higgs production cross section in the Domain-Wall SM to the SM one as a function of $m_{\rm KK}$, along with the LHC constraint $R_{gg} \leq 1.19$ (dashed line). Right: The signal strength of the process $gg \to h \to \gamma\gamma$ in the Domain-Wall SM, along with the LHC constraint $\mu^{\gamma\gamma} \leq 1.33$ (dashed line).

Similarly, the contribution to $C_{\gamma\gamma}$ from the KK-mode top quarks is given by

$$C_{\gamma\gamma}^{\rm KK-top} \simeq \frac{\alpha_{\rm em}}{6\pi v} b_1^t \frac{\partial}{\partial \log v} \log(m_{\rm KK}) \times 2 \simeq \frac{4\alpha_{\rm em}}{9\pi v} \left(\frac{m_t}{m_{\rm KK}}\right)^2, \tag{4.51}$$

where $b_t^t = 4/3$ is a top quark contribution to the QED beta function coefficient. In calculating the contribution from the KK-mode W boson, we consider the expansion in Eq. (4.19) with $m_V = m_\varphi$ to simplify our analysis. In this case, the 1st KK-mode W boson has mass $\sqrt{\left(m_W^{(1)}\right)^2 + m_W^2} \simeq m_{\rm KK}$, and we find the contribution to $C_{\gamma\gamma}$ from the KK-mode W boson as

$$C_{\gamma\gamma}^{\rm KK-W} \simeq \frac{\alpha_{\rm em}}{8\pi v} b_1^W \frac{\partial}{\partial \log v} \log\left(\sqrt{\left(m_W^{(1)}\right)^2 + m_W^2}\right) \simeq -\frac{7\alpha_{\rm em}}{8\pi v} \left(\frac{m_W}{m_{\rm KK}}\right)^2, \tag{4.52}$$

where $b_1^W = -7$ is the W-boson contribution to the QED beta function coefficient.

At the LHC, the Higgs boson is dominantly produced via gluon fusion process. Let us now evaluate the ratio of the Higgs production cross section in the presence of the KK-modes to the SM one as

$$R_{gg} = \frac{\sigma(pp \to h)_{\rm DMSM}}{\sigma(pp \to h)_{\rm SM}} = \left(1 + \frac{C_{gg}^{\rm KK-top}}{C_{gg}^{\rm SM}}\right)^2. \tag{4.53}$$

This ratio as a function of $m_{\rm KK}$ is shown in Figure 4.3 (left panel). In the presence of the KK-mode top quarks, the Higgs production cross section through the gluon fusion channel is altered from the SM prediction. This deviation becomes larger as $m_{\rm KK}$ is lowered. Since the Higgs boson properties measured by the LHC experiments are found to be consistent with the SM predictions [71], we can obtain a lower bound on $m_{\rm KK}$ from the LHC results. Employing the results from a combined analysis by the ATLAS and the CMS collaborations [71], $0.89 \leq R_{gg} \leq 1.19$, we can read off a lower bound as $m_{\rm KK} \geq 799$ GeV from the left panel of Figure 4.3.

The ratio of the partial decay width of $h \to \gamma\gamma$ in our model to the SM one is given by

$$R_{\gamma\gamma} = \frac{\Gamma(h \to \gamma\gamma)_{\rm DMSM}}{\Gamma(h \to \gamma\gamma)_{\rm SM}} = \left(1 + \frac{C_{\gamma\gamma}^{\rm KK-top} + C_{\gamma\gamma}^{\rm KK-W}}{C_{\gamma\gamma}^{\rm SM}}\right)^2 . \tag{4.54}$$

Using this formula, we calculate the signal strength of the process $gg \to h \to \gamma\gamma$ in our model as

$$\mu^{\gamma\gamma} = \frac{\sigma(gg \to h \to \gamma\gamma)}{\sigma(gg \to h \to \gamma\gamma)_{\rm SM}} \simeq R_{gg} \times R_{\gamma\gamma}, \tag{4.55}$$

where we have used the branching ratio to ${\rm BR}(h \to \gamma\gamma) \ll 1$. The right panel in Figure 4.3 shows the signal strength as a function of $m_{\rm KK}$, along with the LHC constraint of $0.96 \leq \mu^{\gamma\gamma} \leq 1.33$, from the ATLAS and CMS combined analysis [71]. We read off a lower bound as $m_{\rm KK} \geq 552$ GeV from the right panel of Figure 4.3, which is milder than the lower bound obtained from the R_{gg} result.

The SM Higgs boson is accompanied by a KK-mode Higgs boson which couple with a top quark pair, as we have seen in Eqs. (4.41) and (4.42). Hence, the KK-mode Higgs boson can be produced at the LHC through the gluon fusion. The coupling of the KK-mode Higgs boson to top quarks can be enhanced for a large x_0 (see the left panel of Figure 4.1). It would be worth investigating the LHC phenomenology for the KK-mode Higgs boson.

4.5.3 Phenomenology of KK-mode fermions

Let us consider interactions between the SM fermions and their KK-modes. Since the eigenfunctions of the SM gauge bosons, which are the zero-modes, are independent of y, an interaction among one SM fermion, one KK-mode fermion and one SM gauge boson vanishes by the orthogonal condition for the eigenfunctions. This is also true for a Yukawa interaction among one SM fermion, one KK-mode fermion and one SM Higgs boson, if the SM SU(2) doublet and singlet fermions are decomposed by the same KK-mode eigenfunctions, as we have considered in this chapter to simplify our discussions. However, there is a unique interaction between an SM fermion and its KK-mode derived from the Yukawa interaction with the kink scalar in Eq. (3.23),

$$\begin{aligned}\mathcal{L} &\supset Y\varphi\left(\overline{\psi_L}\psi_R + \overline{\psi_R}\psi_L\right) \\ &\supset Y\frac{3m_\varphi}{2}\sqrt{\frac{m_\varphi}{2}}\left[\frac{1}{\cosh^5(m_\varphi(y-y_0))}\right]\varphi^{(0)}(x)\overline{\psi_L^{(0)}(x)}\psi_R^{(1)}(x) + \text{H.c.},\end{aligned} \tag{4.56}$$

where we have used the KK-mode expansions in Eqs. (4.33) and (4.34) with the shift of the kink center to $y = 0 \to y_0$. Integrating out the 5th dimensional degrees of freedom, we obtain a 4D effective interaction,

$$\mathcal{L}_{\text{eff}} \supset y_{\text{eff}}\,\varphi^{(0)}\overline{\psi_L^{(0)}}\psi_R^{(1)} + \text{H.c.}, \tag{4.57}$$

where

$$y_{\text{eff}} = \frac{3m_\varphi}{2}\sqrt{\frac{m_\varphi}{2}}\int_{-\infty}^{\infty}\frac{dy}{\cosh^5(m_\varphi(y-y_0))} = Y\frac{9\pi}{16}\sqrt{\frac{m_\varphi}{2}}. \tag{4.58}$$

Therefore, the KK-mode fermion decays to the zero-mode fermion and the massless scalar, the NG boson associated with the breakdown of 5th dimensional translational invariance.

In the extension to the SM case, we identify the fermions in Eq. (4.57) with an SM fermion and it's "KK-mode partner." This Yukawa interaction leads to an interesting

phenomenology for the KK-mode fermions. At the LHC, a pair of KK-mode fermions can be produced through gauge interactions. For example, we may consider a pair of KK-mode quarks produced through gluon fusion. Once a KK-mode fermion is produced, it decays into an SM fermion and the SM-singlet NG boson $\varphi^{(0)}$. Hence, a characteristic signature of the process at the LHC is a final state with two SM fermion jets and a missing energy from $\varphi^{(0)}$s. Note that this is analogous to a signature of superparticle pair production in the simplified supersymmetric models [75], where a superparticle produced in pair decays to its partner SM particle and a stable neutralino. In order to obtain the current LHC constraints on KK-mode quarks, for example, we may apply the ATLAS and CMS results from the search for squarks with a process $pp \to \tilde{q}\bar{\tilde{q}}$, followed by $\tilde{q} \to q\tilde{\chi}_1^0$. A massless limit for neutralino corresponds to our case. Although the production cross section for KK-mode quarks is a few times larger than that for squarks, we roughly obtain $m_{\rm KK} \gtrsim 1.5$ TeV for the KK-mode quarks from the current LHC results [76].

4.6 Conclusions and discussions

In this chapter, we have investigated aspects of the Domain-Wall SM in detail. For concreteness, we have introduced two solvable examples to localize all the SM particles in certain domains of the 5th dimension, and have explicitly shown the KK-mode mass spectrum and eigenfunctions. One example predicts an infinite tower of the KK-mode of the SM gauge bosons, while the number of KK-modes is finite in the other example. With explicit forms of the KK-mode eigenfunctions, we have derived the 4D effective Lagrangian involving the KK-mode SM particles. The Domain-Wall SM offers a variety of interesting phenomenologies. Among others, we have addressed, in this chapter, the LHC phenomenology of the KK-mode gauge boson, the effect of the KK-mode SM fermions on Higgs boson phenomenology, and the KK-mode fermion search at the LHC with its decay into a corresponding SM fermion and a NG boson associated with a spontaneous breaking of the translational invariance in the 5th dimension.

In our solvable examples, we have introduced a special function $s(y)$ to localize the 5D gauge field, as well as the 5D Higgs field and its VEV. In the theoretical point of view, we may seek a possible origin of $s(y)$. The second example of Eq. (4.10) is particularly interesting, since it is expressed in terms of the kink solution when $m_V = m_\varphi$,

$$s(y) = \frac{M}{[\cosh(m_\varphi y)]^{2\gamma}} = M\left(1 - \frac{\sqrt{\lambda}}{m_\varphi}\,\varphi_{\rm kink}(y)^2\right)^\gamma . \tag{4.59}$$

In the normal field theory sense, the parameter γ is an integer. Since a KK-mode exists for $\gamma > 1$, we are interesting in the choice of $\gamma \geq 2$. Now we propose a unified picture of localizing all the SM fields by

$$s(y) = M_G\left(1 - \frac{\sqrt{\lambda}}{m_\varphi}\,\varphi_{\rm kink}(y)^2\right)^{\gamma_G}, \quad s_H(y) = M_H\left(1 - \frac{\sqrt{\lambda}}{m_\varphi}\,\varphi_{\rm kink}(y)^2\right)^{\gamma_H}, \tag{4.60}$$

where $M_{G,H}$ are positive mass parameters, and $\gamma_{G,H}$ are integers. Note that this picture also introduces interactions between the physical modes in φ and the gauge bosons. This phenomenology is worth considering.

In our analysis, we have implicitly assumed that all the SM fermions have the same domain-wall configuration. However, in general, SM chiral fermions can be localized around different points. Such a generalization opens up a possibility to solve the fermion mass hierarchy problem in the SM from the wave-function overlapping, leading to an exponentially suppressed effective Yukawa coupling, as proposed in Ref. [31]. Configurations of the domain-wall fermions reflect their effective gauge couplings with the KK-mode gauge bosons. Therefore, this "geometry" relating to the fermion mass hierarchy can be tested at the future LHC experiment, once a KK-mode gauge boson is discovered and its branching ratios into final state fermions are measured.

CHAPTER 5

FERMION MASS HIERARCHY AND PHENOMENOLOGY IN THE 5D DOMAIN WALL STANDARD MODEL

5.1 Introduction

In this chapter, one of the main pursuits is to explain the mass hierarchy of the fermions, by utilizing the setup of the 5D Domain-Wall SM in Ref. [33]. As has been originally proposed in Ref. [31], the fermion mass hierarchy can be naturally explained by "geometry", namely, localizing the fermions in different positions along the extra dimension. In this "split fermion scenario", the effective 4D Kaluza-Klein (KK) mode gauge couplings to the SM fermions become non-universal due to the different fermion localization points. As a result, the scenario is severely constrained by the Flavor Changing Neutral Current (FCNC) measurements. Detailed analysis for the FCNC constraints has been performed in Ref. [78]. Following their analysis, we consider the current FCNC constraints to identify the allowed parameter region of our model. We also consider the Large Hadron Collider (LHC) Run-2 results from the search for a narrow resonance and interpret the LHC results into the constraints on the KK-mode gauge boson. We find two separate scenarios to satisfy the experimental constraints: (1) the KK modes of the SM gauge bosons are extremely heavy and unlikely to be produced at the LHC, while improved FCNC measurements in the near future can reveal the existence of these heavy modes. (2) the width of the localized SM fermions is very narrow and the 4D KK-mode gauge couplings become almost universal. In this case, the FCNC constraints can be easily avoided even if a KK gauge boson mass is at the TeV scale. Such a light KK gauge boson

can be searched at the LHC Run-3 and the High-Luminosity LHC in the near future.

This chapter is organized as follows: In Sec. 5.2 we utilize the second solvable example for s(y) from [33] and give the corresponding localized gauge field solutions, which will be used throughout this chapter. In Sec. 5.3 we briefly discuss how to extend the domain-wall (DW) Higgs mechanism to the SM gauge group. Sec. 5.4 focuses on the DW SM fermion, and we show how to reproduce the fermion mass hierarchy through "geometry" without big hierarchies among the original model parameters. In Sec. 5.5 we evaluate the 4D effective gauge couplings between the KK gauge bosons and the SM fermions. This aspect of our model is a crucial element for the phenomenology considerations in the next section, as the non-universal nature of the gauge couplings induces FCNC processes. In Sec. 5.6 we discuss how our model avoids the constraints from the FCNC measurements induced by the non-universal gauge couplings. We also consider the LHC Run-2 results of the search for a narrow resonance and interpret the results into the constraint on the KK-mode SM gauge bosons. We find that two distinct situations arise: either the KK gauge boson is very heavy, or it can be light enough to be produced at the LHC. We summarize our discussion in the last section.

5.2 Domain-wall gauge sector

For our analysis in this chapter, we adopt the second example for $s(y)$ considered in Ref. [33]

$$s(y) = f(y)^2 = \frac{M}{[\cosh(m_V y)]^{2\gamma}}, \tag{5.1}$$

where M and m_V are positive mass parameters, and γ is a positive constant.

For our discussion, let us fix $\gamma = 3$. In this case, we have only two KK modes present with the mass eigenvalues $m_1^2 = 5m_V^2$ and $m_2^2 = 8m_V^2$. The canonically normalized

KK-mode expansions are found to be

$$A_\mu(x,y) = g\,A_\mu^{(0)}(x) + 2\,g\,\sinh(m_V y)\,A_\mu^{(1)}(x) + \frac{g}{\sqrt{5}}\left(5 - 4\cosh^2(m_V y)\right)A_\mu^{(2)}(x),$$
$$A_y(x,y) = \sqrt{\frac{4}{5}}\,g\,\cosh(m_V y)\,\eta^{(1)}(x) + \sqrt{\frac{8}{5}}\,g\,\cosh(m_V y)\sinh(m_V y)\,\eta^{(2)}(x), \qquad (5.2)$$

where the gauge coupling in the 4D effective theory is defined as $g = \sqrt{\frac{15 m_V}{16 M}}$.

5.3 Domain-wall Higgs mechanism

The extension of the 5D Abelian Higgs model to the SM case is straightforward. For the 5D SM gauge bosons corresponding to the $\mathrm{SU}(3)_c \times \mathrm{SU}(2)_L \times \mathrm{U}(1)_Y$ gauge groups, we employ the same function $s(y)$ up to a normalization factor which determines the size of each gauge coupling. Hence, the KK-mode spectrum for the SM gauge bosons are the same. After the electroweak symmetry breaking we find the gauge boson (photon (γ), W boson and Z boson) mass spectrum as follows: For the zero-modes,

$$m_\gamma = 0, \;\; m_W = \frac{1}{2} g_2 v, \;\; m_Z = \frac{1}{2} g_Z v, \qquad (5.3)$$

where $g_Z = \sqrt{g_2^2 + g_Y^2}$ with g_2 and g_Y being the $\mathrm{SU}(2)_L$ and $\mathrm{U}(1)_Y$ gauge couplings, respectively, and $v = 246$ GeV is the Higgs doublet VEV, while their KK-mode mass spectrum is given by

$$m_\gamma^{(n)} = m_n, \;\; m_W^{(n)} = \sqrt{m_n^2 + m_W^2}, \;\; m_Z^{(n)} = \sqrt{m_n^2 + m_Z^2}. \qquad (5.4)$$

The gluon mass spectrum is the same as the photon mass spectrum. Since the KK-mode functions for all the SM gauge bosons are identical (up to normalization factors), there is no mass mixing between the KK modes of photon and Z boson.

5.4 Fermion mass hierarchy from geometry

Recall from the DW fermion localization discussion in [32, 33] that fermion KK-mode equations of motion are given by

$$\begin{aligned}\left[-\partial_y^2 - (Y\varphi_{\rm kink})' + (Y\varphi_{\rm kink})^2\right]\chi_L^{(n)} &= m_n^2\chi_L^{(n)},\\ \left[-\partial_y^2 + (Y\varphi_{\rm kink})' + (Y\varphi_{\rm kink})^2\right]\chi_R^{(n)} &= m_n^2\chi_R^{(n)}.\end{aligned} \tag{5.5}$$

Note that a zero mode only exists for a left-handed fermion in the 4D effective theory. This zero-mode is identified with a left-handed SM fermion. If instead we flip the sign of Y from positive to negative in Eq. (5.5), the right-handed fermion has a zero mode, which is identified as a right-handed SM fermion.

For our phenomenology discussion in Sec. 5.6, let us consider fermions located in close proximity to the kink center. In this case, the normalized zero mode wavefunction (for a left-handed SM fermion) is approximately described as

$$\psi_L^{(0)}(x,y) = \psi_L(x)\chi_L^{(0)}(y) \approx \psi_L(x)\left[\left(\frac{m_F^2}{\pi}\right)^{\frac{1}{4}} e^{-\frac{1}{2}m_F^2(y-y_0)^2}\right], \tag{5.6}$$

where $m_F = \sqrt{Ym_\varphi^2/\sqrt{\lambda}}$ is the inverse of the DW fermion width, and we have set the kink center at $y = y_0$. For simplicity, we introduce multiple kink solutions and assume that each 5D fermion couples with its individual kink solution, so that each SM fermion is localized at a different kink center.[1] To simplify our analysis, we set the parameters in kink solutions to yield a common m_F for all SM fermions.

Let us now extend our system to the SM case. We introduce the Yukawa coupling of

[1] Here, the introduction of the multiple kink solutions is not essential. As discussed in the original proposal of the split fermion scenario of Ref. [31], when we introduce a different bulk mass term for each 5D fermion, we can realize the same setup for the localized SM fermions with only one kink solution.

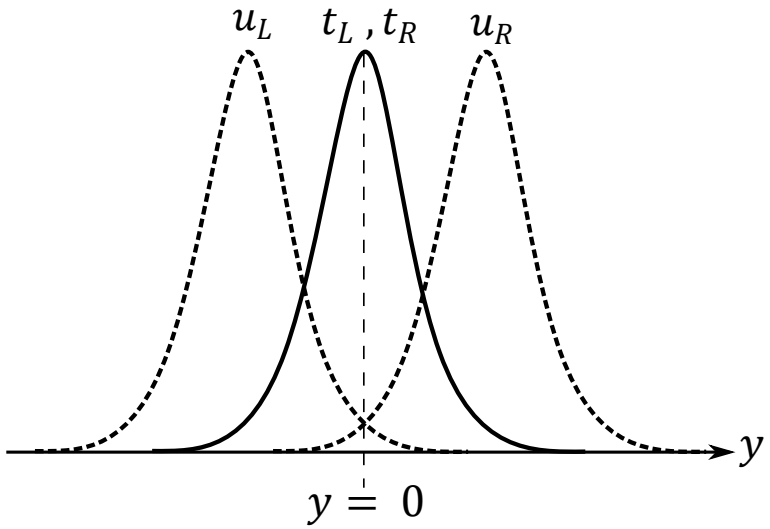

Figure 5.1: The up quark components u_L and u_R are separated by some distance along the 5th dimension, while t_L and t_R are localized at the same location. A small overlap between the chiral fermions results in an exponentially suppressed effective Yukawa coupling.

the SM quarks in 5D as

$$\mathcal{L}_Y = -Y_u^{ij}\overline{Q}^i\tilde{H}u^j - Y_d^{ij}\overline{Q}^i H d^j + \text{H.c.} \supset -Y_u^{ij}\overline{Q}_L^i\tilde{H}u_R^j - Y_d^{ij}\overline{Q}_L^i H d_R^j + \text{H.c.}, \tag{5.7}$$

where we have decomposed the fields into their chiral components $Q^i = Q_L^i + Q_R^i$, $u^i = u_L^i + u_R^i$, $d^i = d_L^i + d_R^i$ ($i = 1, 2, 3$ is the generation index), and H ($\tilde{H} = i\sigma_2 H$) is the 5D Higgs doublet. With the kink background, zero-modes of Q_L^i, and u_R^i/d_R^i are identified with left-handed quark doublet and right-handed quark singlets. The zero mode wavefunctions for Q^i and u^i/d_R^i are given by Eq. (5.6), with the localization positions being different for each SM fermion.

Since the zero mode for the Higgs field and its VEV are flat along the extra dimension ($\chi_h^{(0)}(y) =$ constant in Eq. (4.41)), the effective 4D Yukawa couplings are obtained by integrating out the zero mode quark wavefunctions with respect to the 5th dimensional coordinate. For example, the effective Yukawa coupling of the up-type quarks

is given by

$$Y_{\rm eff}^{ij} = Y_u^{ij} \int_{-\infty}^{\infty} dy\, \chi_L^{i(0)}(y - y_L)\, \chi_R^{j(0)}(y - y_R), \tag{5.8}$$

where the zero modes of the left-handed and right-handed up-type quarks are represented by $\chi_L^{i(0)}(y - y_L)$ and $\chi_R^{j(0)}(y - y_R)$, respectively, are localized at y_L and y_R in the 5th dimension. Note that the effective 4D Yukawa coupling is determined by the amount of overlapping between the left-handed and right-handed zero mode wavefunctions. Figure 5.1 illustrates an example between the chiral components of the up and top quarks. For the chiral components of the zero mode wavefunctions of the top quarks localized at $y = 0$, they completely overlap with each other, and hence the effective Yukawa coupling is identical to the original Yukawa coupling. On the other hand, the chiral components for the zero mode wavefunctions of the up quarks are localized at different positions, resulting in a highly suppressed effective Yukawa coupling. For the present example, we obtain the effective 4D Lagrangian for the mass terms from Eq. (5.7):

$$\begin{aligned} \mathcal{L}_Y^4 \supset & -\frac{v}{\sqrt{2}} \Big(Y_u^{33} \overline{t_L} t_R + Y_u^{11} e^{-m_F^2 (\Delta L_{11}^u)^2}\, \overline{u_L} u_R \\ & + Y_u^{31} e^{-m_F^2 (\Delta L_{31}^u)^2}\, \overline{t_L} u_R + Y_u^{13} e^{-m_F^2 (\Delta L_{13}^u)^2}\, \overline{u_L} t_R \Big), \end{aligned} \tag{5.9}$$

where $\Delta L_{ij}^u = |y_L^i - y_R^j|$. Note that even if $Y_u^{ij} = \mathcal{O}(1)$, the fermion mass hierarchy can be easily reproduced thanks to the geometric factor, $e^{-m_F^2 (\Delta L_{ij}^u)^2}$. The origin of the mass hierarchy is now to be interpreted as a mere factor difference among the ΔL's.

The mass matrices for the up-type and down-type quarks are given by $M_u^{ij} = Y_u^{ij} (v/\sqrt{2}) e^{-m_F^2 (\Delta L_{ij}^u)^2}$ and $M_d^{ij} = Y_d^{ij} (v/\sqrt{2}) e^{-m_F^2 (\Delta L_{ij}^d)^2}$, respectively. The unitary rotations, $u_L^i \to U_L^{ij} u_L^j$, $d_L^i \to V_L^{ij} d_L^j$, and similarly for $L \leftrightarrow R$, diagonalize these mass

matrices as follows:

$$\begin{aligned} \mathrm{diag}(m_u, m_c, m_t) &= U_L^\dagger M_u U_R, \\ \mathrm{diag}(m_d, m_s, m_b) &= V_L^\dagger M_d V_R. \end{aligned} \tag{5.10}$$

The quark mixing matrix (V_{CKM}) is defined as $V_{CKM} = U_L^\dagger V_L$. In order to reproduce the experimentally measured fermion mass values, we assume that the matrices M_u and M_d are Hermitian, so that $U_L = U_R$ and $V_L = V_R$, respectively. Since the up-type quarks mass eigenvalues have a much more hierarchical structure as compared to the down-type quark mass eigenvalues, we approximate $M_u \approx \mathrm{diag}(m_u, m_c, m_t)$. Thus, $U_L = U_R \approx \mathbf{1}$ and $V_L = V_R \approx V_{CKM}$. We fix the top quark Yukawa coupling to be $Y_u^{33} = Y_t = 0.995$ corresponding to $m_t = 173$ GeV, while we take a mild hierarchy choice and assign all remaining Yukawa elements as $0.1\, Y_t$. The separation distance $\Delta L_{ij} = |y_L^i - y_R^j|$ between the left- and right-handed fermions are fixed by their measured masses and found from using Eq. (5.10). The localization positions of the fields are a free parameter so long as the separation distance is satisfied. In our analysis, we have made the choice of left- and right-handed localization positions to be $y_L = \Delta L/2$ and $y_R = -\Delta L/2$. For example, the left-handed and right-handed top quarks are localized at $y = 0$. We employ the same procedure for finding the fermion masses of the lepton sector, where the rotation matrices for the charged leptons and neutrinos are, respectively, $\tilde{U}_L = \tilde{U}_R \approx \mathbf{1}$ and $\tilde{V}_L = \tilde{V}_R \approx V_{PMNS}$. We assume the normal hierarchy of the light neutrino mass spectrum.

5.5 Effective gauge couplings

Let us now describe the interaction Lagrangian in the 4D effective theory as

$$\mathcal{L}_4 \supset \overline{\psi}_L^{(0)} i\gamma^\mu \left(\partial_\mu - iQ_f g A_\mu^{(0)}\right) \psi_L^{(0)} + \sum_{n=1}^{\infty} Q_f\, g_{\text{eff}}^{(n)}\, A_\mu^{(n)} \left[\overline{\psi}_L^{(0)} \gamma^\mu \psi_L^{(0)}\right], \tag{5.11}$$

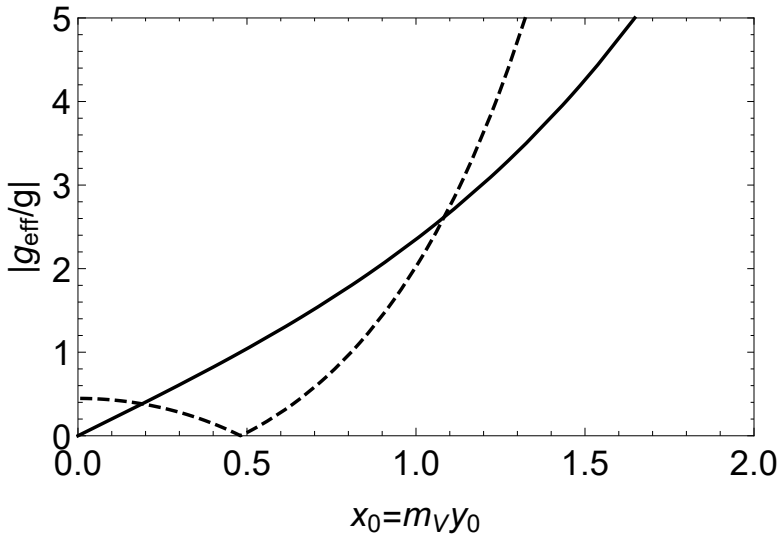

Figure 5.2: Magnitude of effective gauge coupling for the 1st KK (solid line) and the 2nd KK (dashed line) modes as a function of fermion localization position. Here, we have taken $\epsilon = 1$.

where the 4D effective gauge coupling between the chiral fermion and the n-th KK-mode gauge boson is found by integrating out the zero mode function of the fermion and the n-th KK-mode gauge boson function. As an example, the effective gauge coupling of a left-handed SM fermion is given by

$$g_{\rm eff}^{(n)i}/g = \int_{-\infty}^{\infty} dy \left(\chi_L^{(0)i}(y - y_L)\right)^2 \chi^{(n)}(y). \tag{5.12}$$

The effective couplings of the 1st and 2nd KK modes are given by

$$\begin{aligned}
\text{1st KK mode}: \; g_{\rm eff}^{(1)}/g &= \frac{2}{\sqrt{\pi}}\, m_F \int_{-\infty}^{\infty} dy\, \sinh(m_V y)\, e^{-m_F^2 (y-y_L)^2} \\
&= \frac{2}{\sqrt{\pi}} \int_{-\infty}^{\infty} dx\, \sinh(\epsilon x)\; e^{-(x-x_L)^2} \approx 2\epsilon x_L, \\
\text{2nd KK mode}: \; g_{\rm eff}^{(2)}/g &= \frac{1}{\sqrt{\pi}}\, \frac{m_F}{\sqrt{5}} \int_{-\infty}^{\infty} dy\, (5 - 4\cosh(m_V y)^2)\, e^{-m_F^2 (y-y_L)^2} \\
&= \frac{1}{\sqrt{5\pi}} \int_{-\infty}^{\infty} dx\, \left(5 - 4\cosh(\epsilon x)^2\right)\; e^{-(x-x_L)^2} \\
&\approx \frac{1}{\sqrt{5}} \left(1 - 2\left(1 + 2x_L^2\right)\epsilon^2\right),
\end{aligned} \tag{5.13}$$

where $\epsilon = m_V/m_F$, and we have taken $\epsilon \ll 1$ for the final expression of the two equations in order to simplify the formulas. We show these effective couplings in Fig. 5.2 as a function of localization position in the bulk, where we have taken $\epsilon = 1$ for illustrative purposes. For fermions localized at $x_L = m_F y_L = m_V y_L$ near the origin, the effective gauge coupling for the 1st KK-mode is vanishingly small, since the 1st KK-mode function is an odd function of y. Near the origin, the effective coupling of the 2nd KK-mode attains a constant value of $g^{(2)}_{\rm eff}/g \approx 1/\sqrt{5}$, since the 2nd KK-mode function is an even function of y.

5.6 FCNC constraints and KK-mode phenomenology

Prediction of the KK modes in the 4D effective theory is a common property of extra-dimensional models, and we can consider some fascinating phenomenology for them. In the Domain-Wall SM, the KK-mode spectra and the coupling manner of each KK-mode with the SM particles depend on the localization mechanism. This property is in sharp contrast to, for example, the Universal Extra-Dimension model [61], where the KK-mode gauge couplings are universal. The localization of the gauge fields offers more variety of the KK-mode phenomenologies than usual compactified extra-dimensional models, thanks to the rich "geometry" structure of the localized SM particles and their KK modes. In this section, we address two separate scenarios for studying interesting KK-mode phenomenologies: (1) the KK-mode of the SM gauge bosons are extremely heavy and unlikely to be produced at the LHC, while the improved FCNC measurements in the future experiments can reveal the existence of these heavy modes (Sec. 5.6.1). (2) the width of the localized SM fermions is very narrow and as a result, the 4D KK-mode gauge couplings are almost universal. In this case, the FCNC constraints can be easily avoided even for a KK gauge boson mass of order TeV. Such a light KK gauge boson can be searched at the LHC in the near future (Sec. 5.6.2).

5.6.1 FCNC constraints

In many extra dimensional models (see, for example Ref. [79]), a successful localization of the SM fermions to reproduce the fermion mass heirarchy can generate dangerous FCNC processes. The split fermion scenario we consider here is no exception, where FCNC processes originate because of the non-universal effective gauge couplings, which are a result of the different fermion locations along the extra dimension. In the split fermion scenario, Lillie and Hewett in Ref. [78] have considered the FCNC effects mediated by the KK-mode gauge bosons for rare meson decays, and neutral-meson mixings to obtain the constraints on the KK gauge boson masses and fermion localization positions. Since the methodology employed in Ref. [78] is general, it is applicable to our Domain-Wall SM, and we follow Ref. [78] to identify the allowed parameter region in our model. In our analysis, we employ the updated experimental constraints on FCNCs in Ref. [80].

Neglecting the mass splitting induced by the electroweak symmetry breaking (see the last paragraph in Sec. 5.3), the KK-mode spectrum for all SM gauge bosons are the same. Thus, we will focus on the KK gluon mediated processes because of its large QCD coupling. For the SM left-handed and right-handed quarks, the interactions with the n-th KK-mode gluon are given by

$$\begin{aligned}\mathcal{L}_{\rm S} &= i\bar{u}_L^i (U_L^\dagger \tilde{g}_L^{(n)} U_L)_{ij} \gamma^\mu G_\mu^{(n)} u_L^j + i\bar{d}_L^i (V_L^\dagger g_L^{(n)} V_L)_{ij} \gamma^\mu G_\mu^{(n)} d_L^j + (L \leftrightarrow R) \qquad (5.14)\\ &\approx i\bar{u}_L^i (\tilde{g}_L^{(n)})_{ij} \gamma^\mu G_\mu^{(n)} u_L^j + i\bar{d}_L^i (V_{CKM}^\dagger g_L^{(n)} V_{CKM})_{ij} \gamma^\mu G_\mu^{(n)} d_L^j + (L \leftrightarrow R),\end{aligned}$$

where we have used $U_{L/R} \approx \mathbf{1}$ and $V_{L/R} \approx V_{CKM}$ in the second line. The non-universal KK gluon gauge couplings $g_L^{(n)}$ and $\tilde{g}_L^{(n)}$ are then given by

$$\begin{aligned}\tilde{g}_L^{(n)} &= \text{diag}\left\{ g_{eff}^{(n)}(y_{u_L}), g_{eff}^{(n)}(y_{c_L}), g_{eff}^{(n)}(y_{t_L}) \right\}\\ g_L^{(n)} &= \text{diag}\left\{ g_{eff}^{(n)}(y_{d_L}), g_{eff}^{(n)}(y_{s_L}), g_{eff}^{(n)}(y_{b_L}) \right\}, \qquad (5.15)\end{aligned}$$

where all of the effective couplings are dependent on the localization positions of the left-handed fermions. The expressions for $g_R^{(n)}$ and $\tilde{g}_R^{(n)}$ are analogous to Eq. (5.15). As we have discussed in Sec. 5.4, the localization positions are determined (relatively to a m_F value) so as to reproduce experimental value of the quark masses and their mixing matrix elements. Hence, the non-universal KK gluon gauge couplings are determined once $\epsilon = m_V/m_F$ is fixed.

The most stringent bounds on FCNCs come from the meson oscillation measurements found in Ref. [80]. In Ref. [78] the authors consider the effective 4-Fermi interactions mediated by the KK gluons, and derive a lower mass bound on the 1st KK gluon (m_1) as

$$m_1 \geq \beta\sqrt{F(g_L, g_R)}, \tag{5.16}$$

where β is a parameter with a mass-dimension of one. β is determined by the meson parameters, such as the meson decay constant, the corresponding meson mass, the strong coupling constant, and the meson mass difference. For example, for the $K^0 - \bar{K}^0$ oscillation (which turns out to provide the most stringent FCNC constraint), we find $\beta[\text{TeV}] = 1038$, and $F(g_L, g_R)$ is explicitly given by [78]

$$\begin{aligned} F(g_L, g_R) = &\left\{ \frac{4}{5} \left| \left(V_{CKM}^\dagger \frac{g_L^{(1)}}{g} V_{CKM} \right)_{12} \right|^2 + \frac{1}{40} \left| \left(V_{CKM}^\dagger \frac{g_L^{(2)}}{g} V_{CKM} \right)_{12} \right|^2 + (L \leftrightarrow R) \right\} \\ &+ \left(\frac{1}{4} + \frac{3}{4} \frac{m_K^2}{m_d^2 + m_s^2} \right) \left\{ \frac{4}{5} \left| \left(V_{CKM}^\dagger \frac{g_L^{(1)}}{g} V_{CKM} \right)_{21} \times \left(V_{CKM}^\dagger \frac{g_R^{(1)}}{g} V_{CKM} \right)_{12} \right| \right. \\ &\left. + \frac{1}{40} \left| \left(V_{CKM}^\dagger \frac{g_L^{(2)}}{g} V_{CKM} \right)_{21} \times \left(V_{CKM}^\dagger \frac{g_R^{(2)}}{g} V_{CKM} \right)_{12} \right| + (L \leftrightarrow R) \right\}, \end{aligned} \tag{5.17}$$

where the subscripts indicate the matrix elements. Looking back at the effective couplings in Eq. (5.13), one can easily understand that the terms $\propto |g_{L/R}^{(1)}|^2$ are sub-leading compared to the terms $\propto |g_{L/R}^{(2)}|^2$ for $\epsilon \ll 1$. From numerical calculations, we find that the second

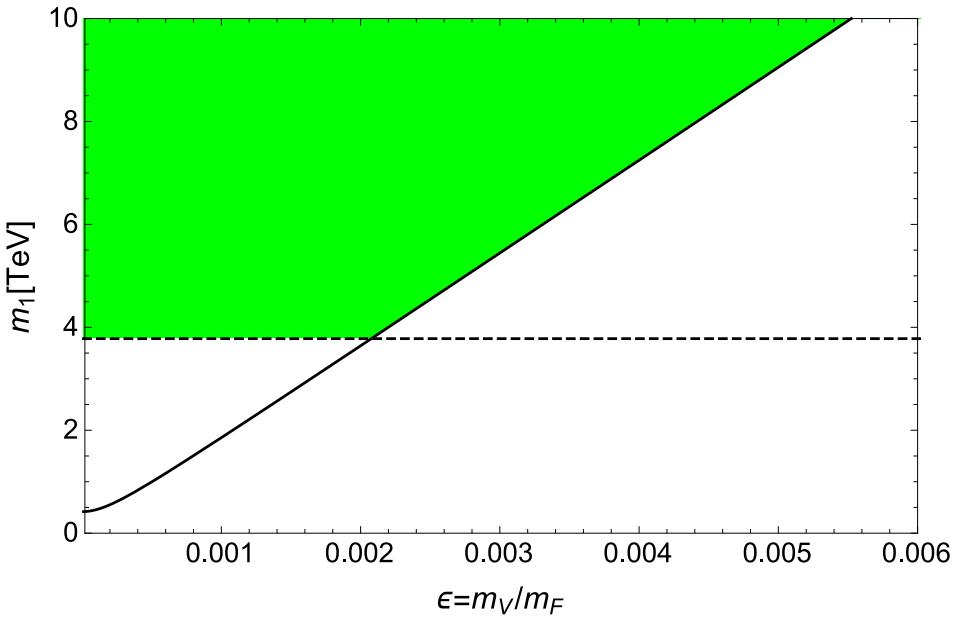

Figure 5.3: The lower bounds on the 1st KK gluon mass (m_1) from the meson oscillation data (diagonal solid line) and the LHC Run-2 results (horizontal dashed lines) as a function of $\epsilon = m_V/m_F$. Combining the two constraints, the allowed region is identified as the green shaded region.

term on the right hand side dominates.

Figure 5.3 shows the lower mass bounds on the 1st KK gluon as a function of ϵ. The diagonal solid line is the constraint obtained from the $K^0 - \bar{K}^0$ oscillation. We have found that the bounds from the B_d^0 and B_s^0 measurements are significantly weaker than the $K^0 - \bar{K}^0$ constraint and we do not show them in the figure. Although our model is not the same as the one examined in Ref. [78], our result is qualitatively consistent with the result presented in Ref. [78]. For $\epsilon \lesssim 0.002$, Fig. 5.3 shows that the FCNC constraints can be avoided even for $m_1 = \mathcal{O}(\text{TeV})$. On the other hand, for a larger ϵ value, the KK gluon must be extremely heavy and far beyond the LHC search reach. The horizontal dashed line is the current lower bound from the LHC Run-2 results. See the next section for details on this constraint.

Typically, rare meson decays place tight constraints on extra dimension models as well, however, in our scenario we have found that these effects are an order of magnitude

weaker than the $K^0 - \bar{K}^0$ oscillation constraint shown in Fig. 5.3. The largest such contribution comes from the process $Br(B_s^0 \to \mu^+\mu^-) = 3 \times 10^{-9}$ [81], from which we have obtained a mass bound on $m_1 \gtrsim 400$ GeV for $\epsilon = 0.004$.

5.6.2 LHC Phenomenology

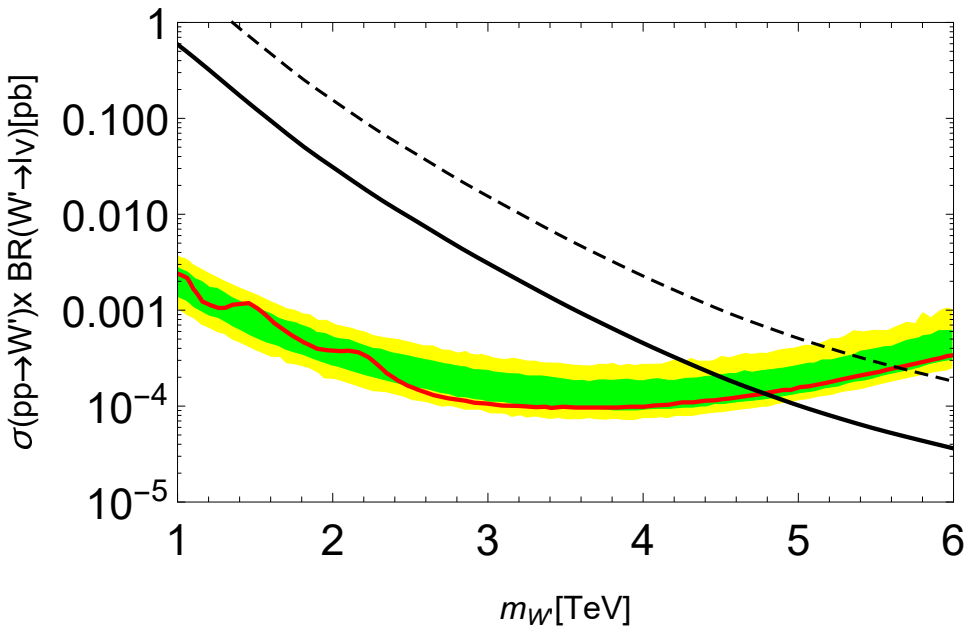

Figure 5.4: The cross section times its branching ratio, $\sigma(pp \to W^{(2)} \to l\nu) = \sigma(pp \to W^(2))\mathrm{BR}(W^{(2)} \to l\nu))$, as a function of $m_{W'} = m_2$ for $g^{(2)}_{\mathrm{eff}}/g = 1/\sqrt{5}$ (solid diagonal line), along with the theoretical prediction of $\sigma(pp \to W' \to l\nu)$ for the sequential SM W' boson (dashed diagonal line) and the cross section upper bound at 95% Confidence Level (solid horizontal curve in red) from the analysis by the ATLAS collaboration with the integrated luminosity of 79.8 fb^{-1} [84]. Here, the 1σ (green) and 2σ (yellow) expected limit bands are also shown.

The ATLAS and the CMS collaborations have been searching for new particle resonances with a variety of final states at the LHC Run-2. For the sequential SM, Z' and W' bosons have the same properties as the SM Z and W bosons except for their masses. The ATLAS (CMS) collaboration has recently reported their search results with luminosity of about 139 fb^{-1} (36 fb^{-1}) for the Z' search, and 80 fb^{-1} (36 fb^{-1}) for the W' search. The ATLAS (CMS) lower bound on the sequential SM Z' boson is obtained to be $m_{Z'} \geq 5.1\,(4.5)$ TeV with dilepton final states [82] ([83]), while $m_{W'} \geq 5.6\,(5.2)$ TeV for the

sequential SM W' boson mass is obtained with its decay mode $W' \to l\nu$ [84] ([85]). In the following, we interpret these results into the constraint on the KK gauge bosons in our model.

Since we have set a common mass m_V for the y-dependent SM gauge couplings, the KK gauge boson mass spectra for gluon, photon, weak bosons are approximately the same for $m_{W,Z}^2 \ll m_1^2 = 5m_V^2$. Thus, we consider the most severe constraint from the W' boson search. Since the total decay width of W' boson is about 3% of its mass for $m_{W'} \gtrsim 1$ TeV, we employ the narrow-width approximation in evaluating the parton-level cross section of the process,

$$\hat{\sigma}(q\overline{q}' \to W') \propto \Gamma_{W'}(W' \to q\overline{q}')\, \delta(M_{\rm inv}^2 - m_{W'}^2) \propto g^2, \tag{5.18}$$

where $M_{\rm inv}^2$ is the invariant mass of the initial partons, $\Gamma_{W'}(W' \to q\overline{q}')$ is the partial decay width into $q\overline{q}'$, and g is the SM SU(2) gauge coupling. When we identify the W' boson with the n-th KK-mode of the SM W boson in the Domain-Wall SM, the only difference is from the effective gauge coupling $g_{\rm eff}^{(n)}$. We have found from Fig. 5.3 that $\epsilon \ll 1$ is required to avoid the FCNC constrains for $m_1 = \mathcal{O}$ (TeV). Since $g_{\rm eff}^{(1)} \propto \epsilon$ for $\epsilon \ll 1$, the 1st KK-mode W-boson production cross section is too small. On the other hand, the 2nd KK-mode W-boson has a sizable coupling, $g_{\rm eff}^{(2)}/g \approx 1/\sqrt{5}$, for $\epsilon \ll 1$, and we use the LHC Run-2 result to obtain a lower mass bound on the 2nd KK-mode. Now, we have a relation,

$$\sigma(pp \to W^{(2)} \to l\nu) = \left(\frac{g_{\rm eff}^{(2)}}{g}\right)^2 \sigma(pp \to W' \to l\nu) \simeq 0.2 \times \sigma(pp \to W' \to l\nu), \tag{5.19}$$

where $\sigma(pp \to W' \to l\nu)$ is the cross section for the sequential W' boson.

In Fig. 5.4, we show the cross section $\sigma(pp \to W^{(2)} \to l\nu)$ as a function of $m_{W'} = m_2$ for the value of $g_{\rm eff}^{(2)}/g = 1/\sqrt{5}$ (solid diagonal line), along with the upper bound on the cross section from the ATLAS results [84] at the LHC Run-2 with a 79.8 fb^{-1} integrated luminosity (horizontal solid curve in red) and the theoretical prediction of

$\sigma(pp \to W' \to l\nu)$ for the sequential SM W' boson (dashed line). We can read off the lower bound on the 2nd KK-mode mass (m_2) from the intersection of the corresponding solid diagonal line and the solid horizontal (red) curve, which is $m_2[\text{TeV}] \geq 4.78$. Considering the ratio between the 1st and 2nd KK gauge boson masses as $m_1/m_2 = \sqrt{5/8}$, we obtain the lower mass bound on the 1st KK gauge boson mass to be $m_1[\text{TeV}] \geq 3.78$. This result is shown in Fig. 5.3 as the horizontal dashed line.

Combining the constraints from the FCNC processes and the LHC Run-2 results, we find the allowed parameter region shown as the green shaded region in Fig. 3. This figure shows two typical regions: (1) $\epsilon \gtrsim 0.002$, for which the FCNC constraints are more severe then the LHC constraint. (2) The LHC constraint is more severe for $\epsilon \lesssim 0.002$. Interestingly, the FCNC and the LHC constraints are complementary to constrain the model parameter space of the Domain-Wall SM.

5.7 Conclusions and discussions

Recently in Refs. [32, 33], we have proposed a framework of the 5D Domain-Wall SM, where all the SM fields are localized in certain 3-dimensional domains in non-compact 5D spacetime. In this chapter, we have extended our previous work to naturally explain the mass hierarchy among the SM fermions by using the idea of the split fermion scenario. Although the fermion mass hierarchy problem can be solved with a mild hierarchy among the model parameters, our model is subject to very severe FCNC constraints. In addition, the current LHC Run-2 narrow resonance search results provide a lower mass bound on the KK-mode SM gauge bosons. Considering the FCNC and the LHC constraints, we have arrived at two typical cases for phenomenological viability of our model: (1) the KK-mode of the SM gauge bosons are extremely heavy and unlikely to be produced at the LHC, while future FCNC measurements can reveal the existence of these heavy modes. (2) the width of the localized SM fermions is very narrow, leading to almost universal 4D KK-mode gauge couplings. In this case, the FCNC constraints can be easily avoided even if

a KK gauge boson mass lies at the TeV scale. Such a light KK gauge boson can be searched at the LHC Run-3 and then the High-Luminosity LHC in the near future. Interestingly, the current experimental constraints from the FCNC measurements and the LHC search for the KK-mode gauge bosons are complementary to constrain parameter space of the Domain-Wall SM.

CHAPTER 6

CONCLUSION

The SM has provided us with an excellent effective theoretical explanation of the fundamental interactions in our current Universe so far, and has been tried and tested by experimentalists to an amazing degree of precision. Despite the robust description of nature the SM has provided, several questions have remained. In particular, the SM has no mechanism with which to tame UV contributions to the Higgs's mass, nor does it give a satisfactory explanation as to how to stabilize the Higgs VEV in the face of quantum corrections. Another aspect of the SM that is not well understood, is the origin behind the SM fermion mass hierarchy. From the expected neutrino mass range, to the top quark mass, lies a energy divide of $\mathcal{O}(10^{13})$ GeV. Developing two separate theoretical frameworks, we have attempted to address these separate issues.

Ameliorating the UV quantum effects to the Higgs boson mass and Higgs self-coupling is key to resolving the hierarchy problem. In chapter 2, based on Ref. [14] we have shown that within the Abelian Higgs model, a Gaussian kinetic operator, which introduces no new poles other than the original theory gives rise to a scale-invariant or a conformal theory in the UV beyond the scale of non-locality. The presence of non-locality arises in the interactions when the vertex operators gain exponential factors in the momentum space, smearing out the vertices. Infinite derivatives are required precisely to make the theory ghost free all the way from IR to UV. In this regard what we have shown is that the beta functions for the Abelian Higgs and the fermion exponentially decreases in the UV beyond the scale of non-locality, essentially making the theory dynamically stable

beyond the non-local scale M. Indeed, the choice of M here is arbitrary. However, it is indicative that in the non-Abelian Higgs, such a new scale, if it appears around $10^{10}10^{11}$ GeV would certainly yield a stable SM Higgs without invoking any new symmetries.

Intrigued by a new approach to localize the SM gauge fields in an extra dimension, in chapter 3 based on Ref. [32] we have proposed a framework to construct Domain-Wall SM which is defined in a non-compact 5D space-time. Considering localization mechanisms for the gauge field, the Higgs field and the chiral fermion in the 5D Minkowski space, we have derived the 4D effective Lagrangian for the SM fields and the gauge boson KK modes. The effective gauge couplings between the KK modes and the SM chiral fermions are controlled by their DW widths. This geometrical property provides us with an interesting LHC phenomenology on the KK modes of the SM gauge bosons, where we've interpreted the current LHC results from the search for a new gauge boson resonance as the constraints on the DWSM.

Developing the theoretical framework of the DWSM even further, in chapter 4 work, based on Ref. [33] we have introduced two solvable examples to localize all the SM particles in certain domains of the 5th dimension, and have explicitly shown the KK-mode mass spectrum and eigenfunctions. One example predicts an infinite tower of the KK modes of the SM gauge bosons, while the number of KK modes are finite in the other example. With explicit forms of the KK-mode eigenfunctions, we have derived the 4D effective Lagrangian involving the KK-mode SM particles. The DWSM offers a variety of interesting phenomenologies including the LHC phenomenology of the KK-mode gauge boson, the effect of the KK-mode SM fermions on Higgs boson phenomenology, and the KK-mode fermion search at the LHC with its decay into a corresponding SM fermion and a NG boson associated with a spontaneous breaking of the translational invariance in the 5th dimension.

Utilizing our previously established theoretical framework for the DWSM in [33], in chapter 5 [34] we have explored the origin of the SM fermion mass hierarchy and shown that two phenomenology scenarios are possible. In the first we've shown that for a heavy

KK gauge gluon, it is still possible to infer the effects of the extra dimension through FCNC considerations. In the second scenario we've shown that no tension exists due to FCNC effects, even given a KK gauge $W^{(2)}$ boson mass on the order of TeV. Such a light KK gauge boson could be discovered at the LHC.

In conclusion, we have shown that through two separate theoretical proposals, we can address two pressing questions that require extensions to the SM. In one proposal, without introducing new particles into the SM, the non-local framework provides a pathway to switch off UV quantum effects. This framework mitigates the effects of the *hierarchy problem* and ensures stability of the Higgs VEV. In our second proposal, through extending our Universe to another flat dimension (5D) and incorporating the effects of "geometry," we have shown that is possible to generate the SM fermion mass hierarchy. Furthermore, after studying the phenomenology of the KK gauge bosons in relation to measurements at the LHC and investigating the tightly constrained FCNC effects, we have established a viable region that may be probed by future experiments.

REFERENCES

[1] G. Aad *et al.*[ATLAS Collaboration] "Observation of a new particle in the search for the Standard Model Higgs boson with the ATLAS detector at the LHC", Phys. Lett. **B716** , 1-29 (2012).

[2] S. Chatrchyan *et al.*[CMS Collaboration] "Observation of a new boson at a mass of 125 GeV with the CMS experiment at the LHC", Phys. Lett. **B716** , 30-61 (2012).

[3] M. Tanabashi *et al.* [Particle Data Group],"11.Status of Higgs Boson Physics", Phys. Rev. D **98**, 030001, pp. 180–228 ,(2018).

[4] E. Gildener, Phys. Lett. **92B**, 1-2 (1980).

[5] C. H. Llewellyn Smith and G. G. Ross , Phys. Lett. **105B**, 1 (1981).

[6] H. E. Haber and G. L. Kane, Phys. Rept. **117**, 75 (1985).

[7] E. Witten, Nucl. Phys. B **185**, 513-554 (1981)

[8] L. Susskind, Phys. Rev. D **20** 10 (1979)

[9] N. Arkani-Hamed, S. Dimopoulos and G. R. Dvali, "The Hierarchy problem and new dimensions at a millimeter," Phys. Lett. B **429**, 263 (1998) [hep-ph/9803315];
I. Antoniadis, N. Arkani-Hamed, S. Dimopoulos and G. R. Dvali, "New dimensions at a millimeter to a Fermi and superstrings at a TeV," Phys. Lett. B **436**, 257 (1998) [hep-ph/9804398].

[10] S. Coleman, Phys. Rev. D **15** 2929 (1977)

[11] R. A. Flores and M. Sher, Phys. Rev. D **27**, 1679 (1983).

[12] M. Sher, Phys. Lett. B **317**, 159 (1993).

[13] M. Sher *et al.*, Phys. Rev. D **91**, 013003 (2015).

[14] A. Goshal, A. Mazumdar, N. Okada, D. Villalba, Phys. Rev. D **97** no.7, 076011 (2018)

[15] E. Witten, "Noncommutative Geometry and String Field Theory," *Nucl.Phys.*, vol. B268, p. 253, 1986.

[16] V. A. Kostelecky and S. Samuel, "On a Nonperturbative Vacuum for the Open Bosonic String," *Nucl.Phys.*, vol. B336, p. 263, 1990.

[17] V. A. Kostelecky and S. Samuel, "The Static Tachyon Potential in the Open Bosonic String Theory," *Phys.Lett.*, vol. B207, p. 169, 1988.

[18] P. G. Freund and M. Olson, "Nonarchimedeanstrings," *Phys.Lett.*, vol. B199, p. 186, 1987.

[19] P. G. Freund and E. Witten, "Adelic String Amplitudes," *Phys.Lett.*, vol. B199, p. 191, 1987.

[20] L. Brekke, P. G. Freund, M. Olson, and E. Witten, "Nonarchimedean String Dynamics," *Nucl.Phys.*, vol. B302, p. 365, 1988.

[21] P. H. Frampton and Y. Okada, "Effective Scalar Field Theory of $P-$adic String," *Phys.Rev.*, vol. D37, pp. 3077–3079, 1988.

[22] A. A. Tseytlin, Phys. Lett. B **363**, 223 (1995)

[23] T. Biswas, M. Grisaru, and W. Siegel, "Linear Regge trajectories from worldsheet lattice parton field theory," *Nucl.Phys.*, vol. B708, pp. 317–344, 2005.

[24] W. Siegel, "Stringy gravity at short distances," hep-th/0309093.

[25] C. Patrignani *et al.* [Particle Data Group], Chin. Phys. C **40**, no. 10, 100001 (2016).

[26] T. Biswas and N. Okada, Nucl. Phys. B **898**, 113 (2015)

[27] M. Tanabashi *et al.* [Particle Data Group],"Quark Summary Table", Phys. Rev. D **98**, 030001, pp. 40 ,(2018).

[28] M. Tanabashi *et al.* [Particle Data Group],"14.Neutrino Masses, Mixing, and Oscillations", Phys. Rev. D **98**, 030001, pp. 251–286 ,(2018).

[29] R. N. Mohapatra and A. Y. Smirnov, Neutrino Mass and New Physics, Ann. Rev. Nucl. Part. Sci. **56**, 569 (2006) [hep-ph/0603118].

[30] L. Randall and R. Sundrum, "A Large mass hierarchy from a small extra dimension," Phys. Rev. Lett. **83**, 3370 (1999) [hep-ph/9905221].

[31] N. Arkani-Hamed and M. Schmaltz, "Hierarchies without symmetries from extra dimensions," Phys. Rev. D **61**, 033005 (2000) [hep-ph/9903417].

[32] N. Okada, D. Raut and D. Villalba, "Domain-Wall Standard Model in non-compact 5D and LHC phenomenology," arXiv:1712.09323 [hep-ph].

[33] N. Okada, D. Raut and D. Villalba, "Aspects of Domain-Wall Standard Model," arXiv:1801.03007 [hep-ph].

[34] N. Okada, D. Raut and D. Villalba, " Fermion Mass Hierarchy and Phenomenology in the Domain Wall Standard Model ,".

[35] R. Davies, D. P. George and R. R. Volkas, "The Standard model on a domain-wall brane," Phys. Rev. D **77**, 124038 (2008) [arXiv:0705.1584 [hep-ph]].

[36] G. R. Dvali and M. A. Shifman, "Domain walls in strongly coupled theories," Phys. Lett. B **396**, 64 (1997) Erratum: [Phys. Lett. B **407**, 452 (1997)] [hep-th/9612128].

[37] K. Ohta and N. Sakai, "Non-Abelian Gauge Field Localized on Walls with Four-Dimensional World Volume," Prog. Theor. Phys. **124**, 71 (2010) Erratum: [Prog. Theor. Phys. **127**, 1133 (2012)] [arXiv:1004.4078 [hep-th]].

[38] V. A. Rubakov and M. E. Shaposhnikov, "Do We Live Inside a Domain Wall?," Phys. Lett. **125B**, 136 (1983).

[39] T. Biswas, A. Mazumdar and W. Siegel, JCAP **0603**, 009 (2006)

[40] T. Biswas, E. Gerwick, T. Koivisto and A. Mazumdar, Phys. Rev. Lett. **108**, 031101 (2012)

[41] A. S. Koshelev and A. Mazumdar, "Absence of event horizon in massive compact objects in infinite derivative gravity," arXiv:1707.00273 [gr-qc].

[42] J. Edholm, A. S. Koshelev and A. Mazumdar, Phys. Rev. D **94**, no. 10, 104033 (2016)

[43] E. Tomboulis, Phys. Lett. B 97, 77 (1980). E. T. Tomboulis, Renormalization And Asymptotic Freedom In Quantum Gravity, In *Christensen, S.m. (Ed.): Quantum Theory Of Gravity*, 251-266. E. T. Tomboulis, Superrenormalizable gauge and gravitational theories, hep- th/9702146.

[44] L. Modesto, Phys. Rev. D 86, 044005 (2012)

[45] S. Talaganis, T. Biswas and A. Mazumdar, Class. Quant. Grav. **32**, no. 21, 215017 (2015)

[46] Zeits., f. Phys.,88, 92 (1934)

[47] G. Efimov Commun. math. Phys. 5, 4256 (1967)

[48] V. Alebastrov and G. Efimov, "A proof of the unitarity of S matrix in a nonlocal quantum field theory," *Commun.Math.Phys.*, vol. 31, pp. 1–24, 1973.

[49] J. Moffat, "Finite nonlocal gauge field theory," *Phys.Rev.*, vol. D41, pp. 1177–1184, 1990.

[50] J. Moffat, "Finite quantum field theory based on superspin fields," *Phys.Rev.*, vol. D39, p. 3654, 1989.

[51] G. Efimov, *Sov. J. Nucl. Phys.*, vol. 4, p. 432, 1966.

[52] G. Efimov, "On the construction of nonlocal quantum electrodynamics," *Annals Phys.*, vol. 71, pp. 466–485, 1972.

[53] J. W. Moffat, "Ultraviolet Complete Quantum Field Theory and Gauge Invariance," arXiv:1104.5706 [hep-th].

[54] A. Mazumdar and J. Rocher, Phys. Rept. **497**, 85 (2011)

[55] P. A. R. Ade *et al.* [Planck Collaboration], Astron. Astrophys. **594**, A13 (2016)

[56] F. L. Bezrukov, M. Shaposhnikov, Phys. Lett. B 659 (2008) 703

[57] J. Polchinski, "Dirichlet Branes and Ramond-Ramond charges," Phys. Rev. Lett. **75**, 4724 (1995) [hep-th/9510017]. I. Antoniadis, N. Arkani-Hamed, S. Dimopoulos and G. R. Dvali, "New dimensions at a millimeter to a Fermi and superstrings at a TeV," Phys. Lett. B **436**, 257 (1998) [hep-ph/9804398].

[58] L. Randall and R. Sundrum, "An Alternative to compactification," Phys. Rev. Lett. **83**, 4690 (1999) [hep-th/9906064].

[59] M. A. Luty and N. Okada, "Almost no scale supergravity," JHEP **0304**, 050 (2003) [hep-th/0209178].

[60] M. Arai, F. Blaschke, M. Eto and N. Sakai, "Localized non-Abelian gauge fields in non-compact extra-dimensions," PTEP **2018**, no. 6, 063B02 (2018) [arXiv:1801.02498 [hep-th]].

[61] T. Appelquist, H. C. Cheng and B. A. Dobrescu, "Bounds on universal extra dimensions," Phys. Rev. D **64**, 035002 (2001) [hep-ph/0012100].

[62] J. Hisano and N. Okada, "On effective theory of brane world with small tension," Phys. Rev. D **61**, 106003 (2000) [hep-ph/9909555].

[63] M. Aaboud *et al.* [ATLAS Collaboration], "Search for new high-mass phenomena in the dilepton final state using 36 fb^{-1} of proton-proton collision data at $\sqrt{s} = 13$ TeV with the ATLAS detector," JHEP **1710**, 182 (2017) [arXiv:1707.02424 [hep-ex]].

[64] M. Aaboud *et al.* [ATLAS Collaboration], "Search for a new heavy gauge boson resonance decaying into a lepton and missing transverse momentum in 36 fb^{-1} of pp collisions at $\sqrt{s} = 13$ TeV with the ATLAS experiment," Eur. Phys. J. C **78**, no. 5, 401 (2018) [arXiv:1706.04786 [hep-ex]].

[65] H. Davoudiasl, J. L. Hewett and T. G. Rizzo, "Bulk gauge fields in the Randall-Sundrum model," Phys. Lett. B **473**, 43 (2000) [hep-ph/9911262].

[66] M. E. Peskin and T. Takeuchi, "Estimation of oblique electroweak corrections," Phys. Rev. D **46**, 381 (1992).

[67] M. Baak, M. Goebel, J. Haller, A. Hoecker, D. Ludwig, K. Moenig, M. Schott and J. Stelzer, "Updated Status of the Global Electroweak Fit and Constraints on New Physics," Eur. Phys. J. C **72**, 2003 (2012) [arXiv:1107.0975 [hep-ph]].

[68] M. Arai, F. Blaschke, M. Eto and N. Sakai, "Grand Unified Brane World Scenario," Phys. Rev. D **96**, no. 11, 115033 (2017) [arXiv:1703.00351 [hep-th]]; M. Arai, F. Blaschke, M. Eto and N. Sakai, "Non-Abelian Gauge Field Localization on Walls and Geometric Higgs Mechanism," PTEP **2017**, no. 5, 053B01 (2017) [arXiv:1703.00427 [hep-th]].

[69] During the completion of our manuscript, we have learned that another group is considering a more general procedure for localized gauge fields, and their results will be reported soon: M. Arai, F. Blaschke, M. Eto and N. Sakai, in preparation.

[70] R. F. Dashen, B. Hasslacher and A. Neveu, "Nonperturbative Methods and Extended Hadron Models in Field Theory. 2. Two-Dimensional Models and Extended Hadrons," Phys. Rev. D **10**, 4130 (1974).

[71] G. Aad *et al.* [ATLAS and CMS Collaborations], "Measurements of the Higgs boson production and decay rates and constraints on its couplings from a combined ATLAS and CMS analysis of the LHC pp collision data at $\sqrt{s} = 7$ and 8 TeV," JHEP **1608**, 045 (2016) [arXiv:1606.02266 [hep-ex]].

[72] F. J. Petriello, "Kaluza-Klein effects on Higgs physics in universal extra dimensions," JHEP **0205**, 003 (2002) [hep-ph/0204067]; N. Maru and N. Okada, "Gauge-Higgs unification at LHC," Phys. Rev. D **77**, 055010 (2008) [arXiv:0711.2589 [hep-ph]].

[73] J. F. Gunion, H. E. Haber, G. L. Kane and S. Dawson, "The Higgs Hunter's Guide," Front. Phys. **80**, 1 (2000).

[74] [ATLAS and CDF and CMS and D0 Collaborations], "First combination of Tevatron and LHC measurements of the top-quark mass," arXiv:1403.4427 [hep-ex].

[75] J. Alwall, M. P. Le, M. Lisanti and J. G. Wacker, "Model-Independent Jets plus Missing Energy Searches," Phys. Rev. D **79**, 015005 (2009) [arXiv:0809.3264 [hep-ph]]; J. Alwall, P. Schuster and N. Toro, "Simplified Models for a First Characterization of New Physics at the LHC," Phys. Rev. D **79**, 075020 (2009) [arXiv:0810.3921 [hep-ph]]; D. Alves *et al.* [LHC New Physics Working Group], "Simplified Models for LHC New Physics Searches," J. Phys. G **39**, 105005 (2012) [arXiv:1105.2838 [hep-ph]].

[76] https://twiki.cern.ch/twiki/bin/view/AtlasPublic/SupersymmetryPublicResults; https://twiki.cern.ch/twiki/bin/view/CMSPublic/PhysicsResultsSUS.

[77] M. Arai, F. Blaschke, M. Eto and N. Sakai, "Localization of the Standard Model via the Higgs mechanism and a finite electroweak monopole from non-compact five dimensions," PTEP **2018**, no. 8, 083B04 (2018) [arXiv:1802.06649 [hep-ph]].

[78] B. Lillie and J. L. Hewett, "Flavor Constraints on Split Fermion Models," Phys. Rev. D **68**, 116002 (2003) [hep-ph/0306193].

[79] S. Khalil and R. Mohapatra, "Flavor violation and extra dimensions," Nucl. Phys. B **695**, 313 (2004) [hep-ph/0402225].

[80] L. Wolfenstein, C. J. Lin, E. Pianori, "Tests of Conservation Laws," http://pdg.lbl.gov/2018/reviews/rpp2018-rev-conservation-laws.pdf

[81] R. Aaij et al. [LHCb Collaboration], "Measurement of the $B_s^0 \to \mu^+\mu^-$ Branching Fraction and Effective Lifetime and Search for $B^0 \to \mu^+\mu^-$ Decays," Phys. Rev. Lett. **118**, 191801 (2017) [hep-ex/1703.05747v2 [hep-ex]].

[82] ATLAS Collaboration, "Search for high-mass dilepton resonances using 139 fb^{-1} of pp collisions at $\sqrt{s} = 13$ TeV with the ATLAS detector," https://atlas.web.cern.ch/Atlas/GROUPS/PHYSICS/PAPERS/EXOT-2018-08/ [arXiv:1903.06248 [hep-ex]].

[83] CMS Collaboration, "Search for high-mass resonances in dilepton final states at $\sqrt{s} =$ 13 TeV," JHEP **2018**, 120 (2018) [arXiv:1803.06292 [hep-ex]].

[84] ATLAS Collaboration, "Search for a new heavy gauge boson resonance decaying into a lepton and missing transverse momentum in 79.8 fb^{-1} of pp collisions at $\sqrt{s} = 13$ TeV with the ATLAS experiment," http://cds.cern.ch/record/2621303/.

[85] CMS Collaboration, "Search for high-mass resonances in final states with a lepton and missing transverse momentum at $\sqrt{s} = 13$ TeV," JHEP **2018**, 128 (2018) [arXiv:1803.11133 [hep-ex]].